Lecture 15: Introduction to Liquefaction; Mechanism and factors causing liquefaction; estimation methods and procedures; Mapping

Topics

- What is liquefaction?
- Consequence of Liquefaction:
- Examples from Past earthquakes:
- Classification of Liquefaction
- Evaluation of Liquefaction Hazards
- Liquefaction Susceptibility
- What is a “loose” soil?
- The Critical Void Ratio Line
- The Steady State Line
- Liquefaction Susceptibility Map
- Identification factors: qualitative susceptibility to liquefaction
- Liquefaction susceptibility of silty and clayey sands (Andrew and Martins, 2000)
- Cyclic Stress Ratio (CSR) and Cyclic Resistance Ratio (CRR) :
- What procedures are preferred for estimating amax at potentially liquefiable sites
- Which peak acceleration should be used?
- Stress Reduction Coefficient (rd)
- The capacity of the soil to resist liquefaction, expressed in terms of CRR.(CSR required to cause liquefaction)
- Evaluation of liquefaction resistance (CRR) :
- SPT -Based Procedure for Evaluating Liquefaction Potential and Remarks on CRR from SPT
- CPT -Based Procedure for Evaluating Liquefaction Potential and Comments Regarding the CPT-Based Procedure
- Vs Criteria for Evaluating Liquefaction Resistance and Comments Regarding the Vs-Based Procedure
- Dilatometer Test (DMT)-Based Procedure for Evaluating Liquefaction Potential
- Factor of safety against liquefaction
- Magnitude Scaling Factor (MSF)
- Final Choice of Factor of safety
- Zone of Liquefaction
- Liquefaction Potential Index

Keywords: *Liquefaction, Causes, Estimation Methods, Mapping*

Topic 1

What is liquefaction?

- Liquefaction (as defined by Castro and Poulos) is a phenomenon wherein a saturated sand subjected to monotonic or cyclic shear loads looses a large percentage of its shear resistance and flows in a manner resembling a liquid.

- Marcuson defines liquefaction as the transformation of a granular material from a solid to a liquefied state as a consequence of increased pore-water pressure and reduced effective stress. This phenomenon occurs most readily in loose to medium dense granular soils that have a tendency to compact when sheared.

- In saturated soils, pore-water pressure drainage may be prevented due to the presence of silty or clayey seam inclusions, or may not have time to occur due to rapid loading such as in the case of seismic loads. In this situation, the tendency to compact is translated into an increase in pore-water pressure. This leads to a reduction in effective stress, and a corresponding decrease of the frictional shear strength.

- The term liquefaction, originally coined by Mogami and Kubo (1953), has historically been used in conjunction with a variety of phenomena that involve soil defomations caused by monotonic, transient, or repeated disturbance of saturated cohhesionless soils under undrained conditions.

- The generation of excess pore pressure under undrained loading conditions is a hallmark of all liquefaction phenomena. The tendency for dry cohensionless soils to densify under both static and cyclic loading is well know.

- When cohensionless soils are saturated, however, rapid loading occures under undrained conditions, so the tendency for densification causes excess pore pressures to increase and effective stresses to decrease.

- Liquefaction is a process that occurs in water-saturated unconsolidated sediment due to shaking. In areas underlain by such material, the ground shaking causes the grains to loose grain to grain contact, and thus the material tends to flow (Fig. 15.1).

- You can demonstrate this process to yourself next time your go the beach. Stand on the sand just after an incoming wave has passed. The sand will easily support your weight and you will not sink very deeply into the sand if you stand still. But, if you start to shake your body while standing on this wet sand, you will notice that the sand begins to flow as a result of liquefaction, and your feet will sink deeper into the sand.

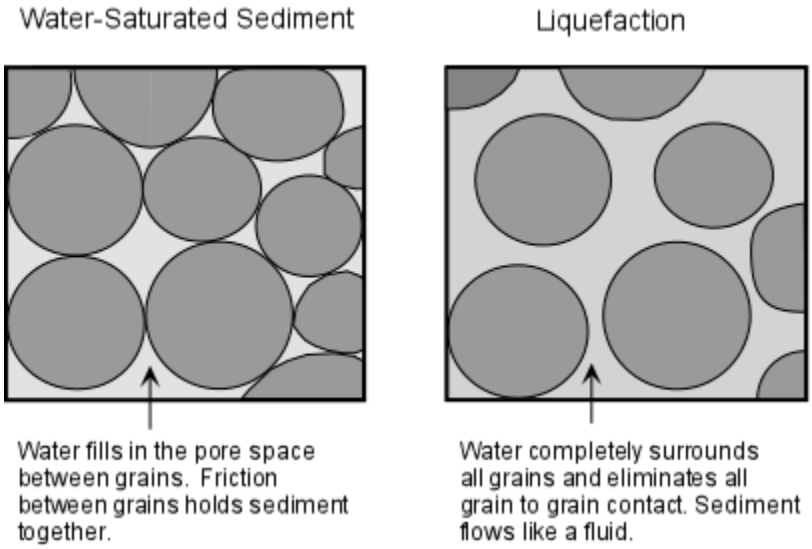

Fig 15.1: Apartment buildings tilted by liquefaction-induced loss of bearing strength during the 1964 Niigata, Japan, earthquake.

Topic 2

Consequence of Liquefaction:

- Liquefaction can cause damage to structures in several ways. Buildings whose foundations bear directly on sand which liquefies will experience a sudden loss of support, which will result in drastic and irregular settlement of the building.

- As liquefied soils lose strength, buildings supported on spread footings can lose bearing capacity and settle or tilt. Buried structures extending below the water can literally "float" out of the ground due to the increased pore water pressures.

- Liquefaction causes irregular settlements in the area liquefied, which can damage buildings and break underground utility lines where the differential settlements are large. Pipelines and ducts may float up through the liquefied sand.

- As the water pressure increases during ground shaking as a result of an earthquake, the ground water may find its way to the ground surface through cracks and vents in the ground to relieve the excess pore pressures. This results in soil particles being carried with the water to the ground surface in what are commonly referred to as "sand boils," looking like small volcanoes with the carried particles stacked up outside of the cracks and vents.

- Sand boils can erupt into buildings through utility openings, and may allow water to damage the structure or electrical systems. Soil liquefaction can also cause slope failures.

- Areas of land reclamation are often prone to liquefaction because many are reclaimed with hydraulic fill, and are often underlain by soft soils which can amplify earthquake shaking.

- Waterfront structures, such as dock or quay walls, would experience greater lateral pressures and may tilt or fail. Buried utilities can be subjected to differential movements along their alignments, and ruptures can occur where the utilities make connections with structures that may move or settle differentially with the utilities.

- Liquefaction can also cause excessive ground oscillations, caused by shaking of unliquefied soils above a deeper liquefied soil layer.

- In addition, liquefaction can result in lateral spreading or flow slides, caused by a surficial layer of soils on a slope (even a very gentle slope) moving downslope over a liquefied soil layer.

Topic 3

Examples from Past earthquakes:

- As listed in Table below, a large number of liquefaction case histories have been documented after earthquakes in China, Japan, South America, and North America. Various types of data have been collected from these case histories and organized into databases (e.g., Seed and Idriss, 1971; Harder, 1991) in an effort to define the evidences for liquefaction (e.g., ground deformations and sand boils) and the circumstances for which liquefaction did occur or did not occur.

- These databases are constantly revised in order to remove possible uncertainties on data collected and add new entries after recent earthquakes. Such databases are the foundation of the engineering liquefaction analyses.

- In these databases, the geometry and properties of soil deposits are mostly characterized by Standard Penetration Tests (SPT), a common soil investigation technique in geotechnical engineering.

- However, new databases have been developed based on other types of soil deposit characteristics including shear-wave velocity (e.g., Andrus et al., 1999) and cone penetration test (CPT) data (e.g., Robertson and Wride, 1998; Stark and Olson, 1995).

Table 15.1: List of Earthquakes with documented case histories of Liquefaction

Earthquake	**Reference**
1891 Mino-Owari, Japan	Kishida (1969)
1906 San Francisco, USA	Hamada and O'Rourke (1992)
1923 Kanto, Japan	Kodera (1964)
1944 Tohnankai, Japan	Kishida (1969)
1948 Fukui, Japan	Kishida (1969)
1960 Tokachi-Oki, Japan	Ohsaki (1970)
1964 Niigata, Japan	Kishida (1969); Koizumi (1966); Ishihara et al. (1979); Youd and Kiehl, (1996)
1971 San Fernando, USA	Hamada and O'Rourke (1992)
1975 Haicheng, China	Xie (1979) ; Shengcong et al. (1983)
1976 Guatemala	Seed et al.(1979)
1976 Tangshan, China	Xie (1979) ; Shengcong et al. (1983)
1977 Argentina	Idriss et al. (1979)
1978 Miyagiken-Oki, Japan	Tohno et al. (1981); Ishihara et al. (1980);
1979 Imperial Valley, USA	Youd and Bennett (1983)
1981 Westmorland, USA	Bennett et al. (1984)
1983 Borah Peak, Idaho	Youd et al. (1985)
1987 Superstition Hills, California	Youd and Holzer (1994); Scott and Hushmand (1995)
1989 Loma Prieta, USA	Holzer (1998) ; Bennet et al. (1999)
1993 Hokkaido Nansei-Oki, Japan	Isoyama (1994)
1994 Northridge earthquake, USA	Holzer et al (1999); Bardet and Davis (1996); Davis and Bardet (1996)

1995 Hyogoken-Nanbu, Japan	Hamada et al. (1996); Ishihara et al.(1996)

- Almost all the case histories on soil liquefaction have been documented after the events took place. There are very few case histories for which the two main factors controlling liquefaction (i.e., pore pressure and ground acceleration) were actually both recorded at the liquefaction sites during earthquakes.

- To our knowledge, only one case history of liquefaction was fully documented with simultaneous acceleration and pore pressure records during an actual earthquake, i.e., at the Wildlife site during the 1987 Imperial Valley earthquake (Holzer et al., 1989).

- A few controversies, however, clouded the measured time history of pore pressure at the Wildlife site (e.g., Scott and Hushmand, 1995; Youd and Holzer, 1994, 1995), and deserve consideration in the analysis of the recordings.

- There have been liquefaction case histories in which the time history of acceleration, but not of pore pressure, was recorded by several downhole strong-motion instruments located at the ground surface and at various depths (i.e., Iwasaki and Tai, 1996), which allowed researchers (e.g., Elgamal et al., 1996) to calculate the average shear-strain behavior of the liquefying soils using inverse methods.

- Several sites throughout the world have now been instrumented with pore pressure sensors, and are likely to yield valuable information on soil liquefaction (e.g., Zeghal and Elgamal, 1994) during future earthquakes.

Topic 4

Classification of Liquefaction

- Robertson (1994) and Robertson et al. (1994) suggested a fairly complete classification system to define "soil liquefaction" and it can be summarized as:

    1. Flow liquefaction, used for the undrained flow of a saturated, contractive soil when the static shear stress exceeds the residual strength of the soil. Failure may be triggered by cyclic or monotonic shear loading.

    2. Cyclic softening used to describe large deformations occurring during cyclic shear due to pore pressure build-up in soils that would tend to dilate in undrained, monotonic shear. Cyclic softening, in which deformations do not continue after cyclic loading ceases, can be further classified as:

a. Cyclic liquefaction, which occurs when cyclic shear stresses exceed the initial, static shear stress to produce a stress reversal. A condition of zero effective stress may be achieved during which large deformations may occur.

b. Cyclic mobility, in which cyclic loads do not yield a shear stress reversal and a condition of zero effective stress, does not develop. Deformations accumulate in each cycle of shear stress.

- This classification system for liquefaction recognizes that various mechanisms may be involved in a given ground failure. Yet, this definition preserves the contemporary usage of the term "liquefaction" to broadly describe the failure of saturated, cohesionless soils during earthquakes.

Topic 5

Evaluation of Liquefaction Hazards

- Areas that may be prone to liquefaction hazard are those that may be subjected to moderate to very strong ground shaking, have young alluvial deposits consisting of sand and silt, and have shallow ground water (within 50 feet of the ground surface).

- Young deposits would be of Holocene to late Pleistocene in age. Geotechnical professionals generally use subsurface exploration techniques to evaluate the potential for liquefaction. The most common technique is to use the Standard Penetration Test blow count (commonly referred to as the "N-value").

- Researchers have developed liquefaction prediction techniques using the expected seismic stresses in the soil from a given design earthquake, and the Nvalue soil resistance.

- If the N-value is great enough, liquefaction would not be expected to occur for a given seismic stress. For sandy soils at sites in the most seismically active areas of the United States, the N-value would generally need to be greater than 30 to not have liquefaction.

- Liquefaction prediction techniques have also been developed based on correlations with Cone Penetration Tests (CPTs). CPTs are becoming more preferred by Geotechnical professionals as they provide essentially continuous soundings of the

soil profile, whereas N-values can only provide discreet resistance values at intervals of several feet.

- Current evaluation techniques can also predict the magnitude of liquefaction-induced settlement. Evaluation techniques are also available to analyze the magnitude of lateral spreading if there are ground slopes.

Topic 6

Liquefaction Susceptibility

- Liquefaction is most commonly observed in shallow, loose, saturated deposits of cohesionless soils subjected to strong ground motions in large-magnitude earthquakes.

- Unsaturated soils are not subject to liquefaction because volume compression does not generate excess pore pressures. Liquefaction and large deformations are more likely with contractive soils while cyclic softening and limited deformations are associated with dilative soils.

- The steady-state concept demonstrates how the initial density and effective confining stress affect the liquefaction characteristics of a particular soil. In practice the potential for liquefaction in a given soil deposit during an earthquake is often assessed using in situ penetration tests and empirical procedures. The most widely accepted procedure for evaluating liquefaction susceptibility, based on the Standard Penetration Test.

- Since liquefaction is associated with the tendency for soil grains to rearrange when sheared, anything that impedes the movement of soil grains will increase the liquefaction resistance of a soil deposit. Particle cementation, soil fabric, and aging - all related to the resistance of a soil deposit. Particle cementation, soil fabric, and aging - all related to the geologic formation of a deposit - are important factors that can hinder particle rearrangement (Seed 1979).

- Soils deposited prior to the Holocene epoch (more than 10,000 years old) are usually not prone to liquefaction (Youd and Perkins 1978), perhaps due to weak cementation at the grain contacts. However, conventional sampling techniques inevitably disturb the structure of cohesionless soils such that laboratory test specimens are usually less resistant to liquefaction than the in situ soil.

- Even with reconstituted laboratory samples, the soil fabric and resistance to liquefaction are affected by the method of preparation such as dry pluviation, moist tamping, water sedimentation, etc. After liquefaction has occurred, the initial soil fabric and cementation have very little influence on the shear strength beyond about 20% strain (Ishihara 1993).

- Stress history also plays an important role in determining the liquefaction resistance of a soil. For example, deposits with an initial static shear stress (anisotropic consolidation conditions) are usually more resistant to pore pressure generation (Seed 1979), although static shear stresses may cause greater deformations once liquefaction occurs. Stress history may also contribute to the liquefaction resistance of older deposits.

- Over consolidated soils, having been subjected to greater static pressures in the past, are more resistant to particle rearrangement and liquefaction. Soil deposits subjected to past cyclic loading are usually more resistant to liquefaction as the soil grains tend to be in a more stable arrangement, but some deposits may be loosened by previous shaking.

- In addition, the frictional resistance between soil grains is proportional to the effective confining stress. Consequently, the liquefaction resistance of a soil deposit increases with depth as the effective overburden pressure increases. For this reason, soil deposits deeper than about 15 m are rarely observed to liquefy (Krinitzsky et al. 1993).

- Characteristics of the soil grains (distribution of sizes, shape, composition, etc.) influence the susceptibility of a soil to liquefy (Seed 1979). While liquefaction is usually associated with sands or silts, gravelly soils have also been known to liquefy. Rounded soil particles of uniform size are generally the most susceptible to liquefaction (Poulos et al. 1985).

- Well-graded sands with angular grain shapes are generally less prone to liquefy because of a more stable interlocking of the soil grains. On the other hand, natural silty sand sediments tend to be deposited in a looser state, and thus are more likely to exhibit contractive shear behavior, than clean sands.

- Clays with measurable plasticity are resistant to the relative movement of particles during cyclic shear loading and are generally not prone to pore pressure generation and liquefaction.

- Plastic fines in sandy soils usually create sufficient adhesion between the sand grains to limit the ability of larger particles to move into a denser arrangement. Consequently, soils with significant plastic fines content are rarely observed to liquefy in earthquakes.

- In contrast, as discussed by Ishihara (1993), non-plastic soil fines with a dry surface texture (such as rock flour) do not create adhesion and do not provide significant resistance to particle rearrangement and liquefaction.

- Moreover, low plasticity fines may contribute to the liquefaction susceptibility of a

soil. Koester (1994) suggests that sandy soils with significant fines content may be inherently collapsible, perhaps due to the greater compressibility of the fines between the sand grains.

- Permeability also affects the liquefaction characteristics of a soil deposit. When pore water movement within a liquefiable deposit is retarded by a low permeability, pore pressures are more likely to accumulate during cyclic loading.

- Consequently, soils with large non-plastic fines content may be more susceptible to liquefaction because the fines inhibit drainage of excess pore pressures. In addition, the liquefaction vulnerability of a soil deposit is affected by the permeability of surrounding soils. Less pervious clayey soils can prevent the rapid dissipation of excess pore pressures generated in an adjacent deposit of saturated sand.

- On the other hand, sufficient drainage above or below a saturated deposit may prevent the accumulation of pore pressures and liquefaction. Due to a relatively high permeability, gravelly soils are less prone to liquefy unless pore water drainage is impeded by less pervious, adjoining deposits.

Topic 7

What is a "loose" soil?

- Loose soils are initially more porous when it is in its natural state and generally, a soil that exhibits contractive behavior upon shearing (Fig.15.2).

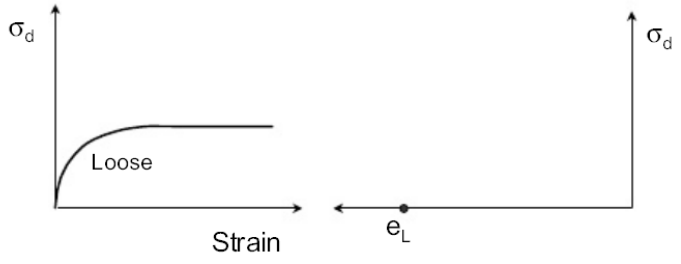

STEP 1

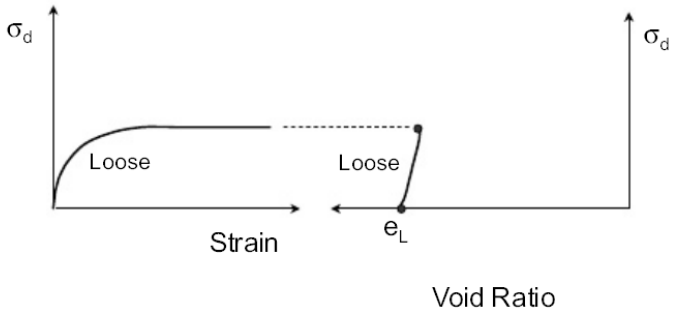

STEP 2

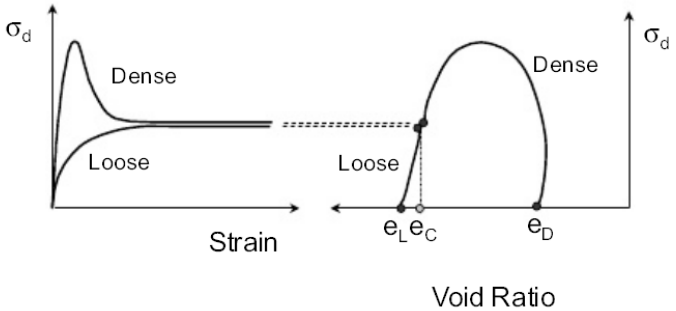

STEP 3

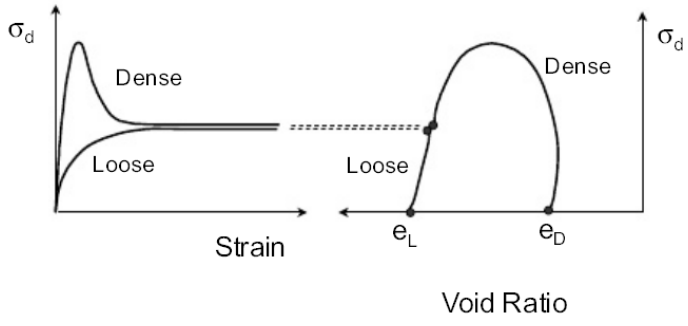

STEP 4

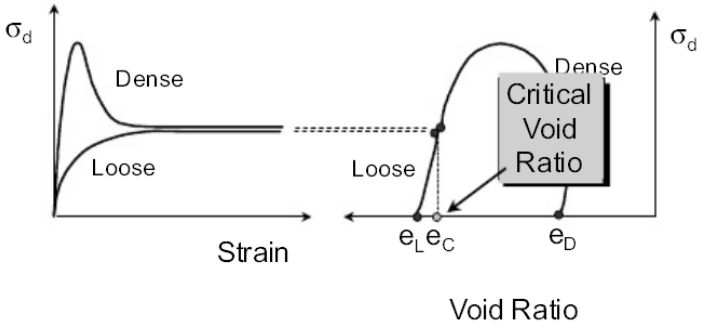

STEP 5

Fig 15.2: Behavior of dense and loose soils in monotonic strain controlled triaxial tests (after Kramer, 1996).

Topic 8

The Critical Void Ratio Line

- In 1936, Dr. Arthur Casagrande performed a series of drained strain-controlled triaxial tests and discovered that initially loose and dense specimens at the same confining pressure approached the same density when sheared to large strains. The void ratio corresponding to this density was called the critical void ratio (e_c).

- Performing tests at various effective confining pressures, Casagrande found that the critical void ratio varied with effective confining pressure. Plotting these on a graph produced a curve which is referred to as the critical void ratio (CVR) line.

- The CVR line constituted the boundary between dilative and contractive behavior in drained triaxial compression. A soil in a state that plots above the CVR line exhibits contractive behavior and vice versa (see figure 15.3).

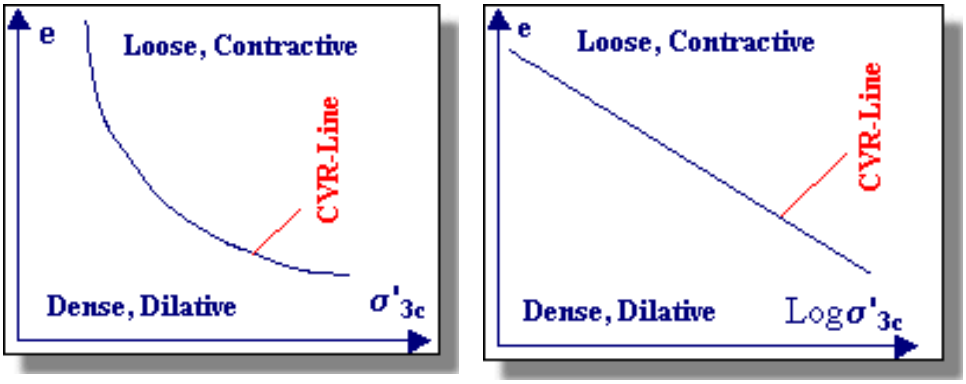

Fig 15.3: CVR-line for arithmetic and logarithmic confining pressure.

Topic 9

The Steady State Line

- In the mid-1960s, Gonzalo Castro, a student of Casagrande, performed an important series of undrained, stress-controlled triaxial tests. Castro observed three different types of stress-strain behavior depending upon the soil state.

- Dense specimens initially contracted but then dilated with increasing effective confining pressure and shear stress. Very loose samples collapsed at a small shear strain level and failed rapidly with large strains. Castro called this behavior "liquefaction" - it is also commonly referred to as flow liquefaction.

- Medium dense soils initially showed the same behavior as the loose samples but, after initially exhibiting contractive behavior, the soil "transformed" and began exhibiting dilative behavior. Castro referred to this type of behavior as "limited liquefaction".

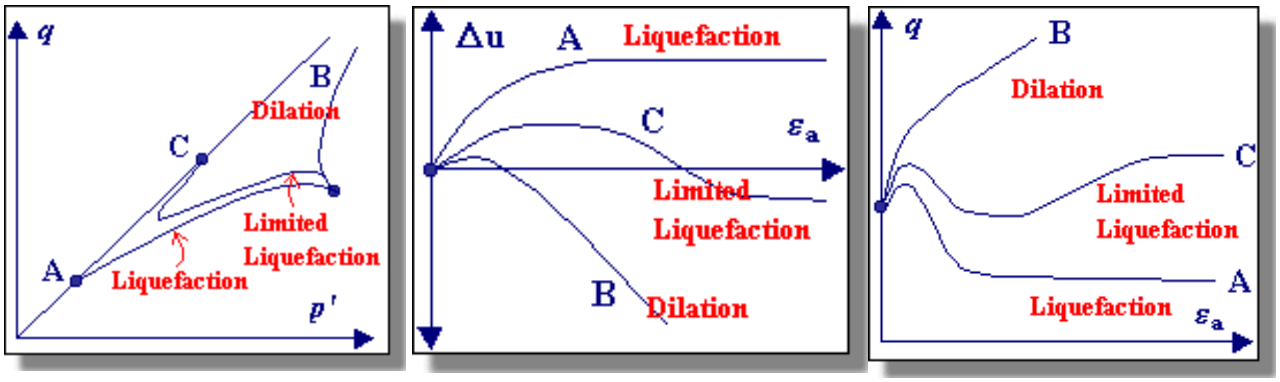

Fig 15.4: Static triaxial test stress paths for three specimens of different densities

- Castro plotted the relationship (see Figure 15.4) between effective confining pressure and void ratio at large strains for these undrained, stress-controlled tests.

Castro referred to the curved produced by this plot, which is similar to the CVR line for the drained strain controlled tests performed by Casagrande, as the Steady State Line (SSL).

- The difference between the CVR and SSL was attributed to the existence of what Casagrande called a "flow structure", in which the grains orient themselves so the least amount of energy is lost by frictional resistance during flow.

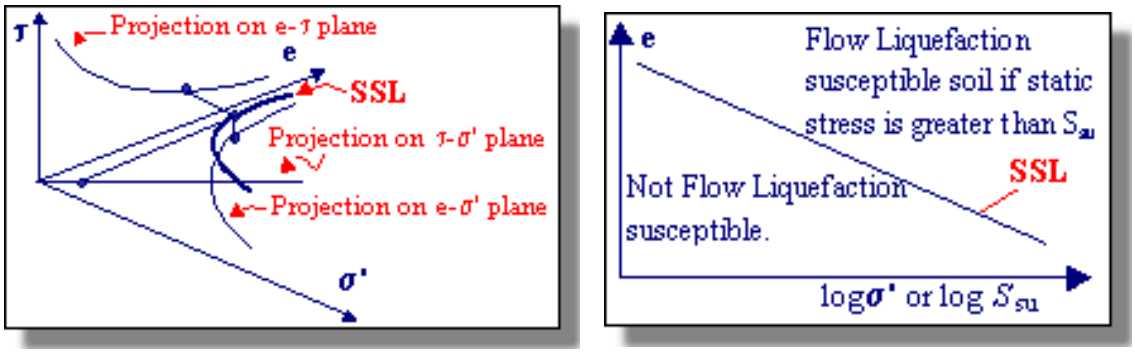

Fig 15.5: Left: 3-D steady state line. Right: 2-D Projection of SSL plotted on graph of void ratio versus the logarithm of confining pressure or steady state strength.

- As seen above, the SSL is actually a 3-dimensional curve in e- s'-t space. Using the 2-D projection on the e-s' plane (see Figure 15.5), one can determine if a soil is susceptible to flow liquefaction(see Figure 15.6).

- Soils in an initial state that plots below the SSL are not susceptible to flow liquefaction whereas soils plotting above the SSL are susceptible to flow liquefaction - if (and only if) the static shear stress exceeds the residual strength of the soil. Cyclic mobility, another liquefaction-related phenomenon, can occur in dense as well as loose soils.

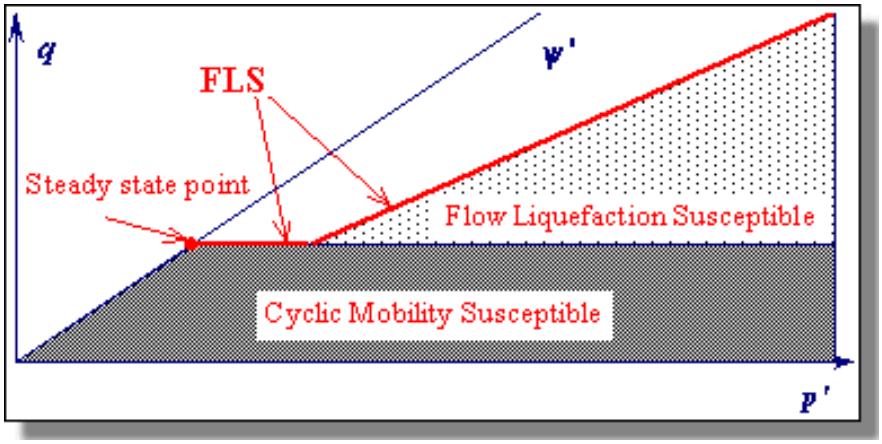

Fig 15.6: showing zones of flow liquefaction and cyclic mobility susceptibility.

Topic 10

Liquefaction Susceptibility Map

- Liquefaction 'susceptibility' is a measure of a soil's inherent resistance to liquefaction, and can range from not susceptible, regardless of seismic loading, to highly susceptible, which means that very little seismic energy is required to induce liquefaction.

- Susceptibility has been evolved by comparing the properties of a given deposits to the other soil deposits where liquefaction has been observed in the past (based on Seed et al, 1985). The primary relevant soil properties considered were grain size, fine content, density, degree of saturation and age of the deposit.

- From Mapping four primary geologic units can be differentiate: Artificial fill, Holocene alluvium, Pleistocene glacio-fluvial outwash, and Pleistocene loess. The results of the integrated analysis show that Holocene alluvial units are the most susceptible to liquefaction.

- Late Pleistocene glacio-fluvial outwash has a moderate-to-low susceptibility; the loess deposits have a very low susceptibility. Artificial fill deposits are common, and are assigned a conservative value of "very high" liquefaction susceptibility because of the difficulties associated with estimating their geotechnical properties, and thus the ability to forecast their response to seismic shaking.

- The maps of liquefaction susceptibility are based on:

    1. Existing and newly completed 1:24,000-scale Quaternary geologic maps for the study area;
    2. Evaluating geologic and geotechnical subsurface borehole information;
    3. Characterizing depth to groundwater data;
    4. Evaluating liquefaction susceptibility incorporating the "Simplified Procedure" devised by Seed and Idriss (1971)

- The Simplified Procedure is a method to estimate the liquefaction susceptibility of a deposit by relating standard penetration test (SPT) blow counts of a soil sample to earthquake-induced cyclic shear stresses, based on liquefaction case history.

- This method is commonly employed because of the volume of SPT data that exists from public engineering projects (e.g. bridges, highways). Other means exist to quantitatively estimate liquefaction susceptibility such as using shear wave velocity (e.g. Andrus and Stokoe, 1999), cone penetration resistance (e.g Mayne, 2000, 2001; Rix, 2001, Tinsley et al., 1985) and Becker penetration test (Youd et al., 2001).

- Because the Simplified Procedure has been extensively used and studied, the method has benefited from revisions and refinements that have improved the level of analysis overall (e.g. Seed et al., 1982, 1983, 1985; Robertson and Wride, 1987; Youd et al., 2001; Idriss and Boulanger, 2004).

- Most recently, Cetin et al. (2004) presented revisions to the Simplified Procedure that are based on updates to the case history database to include new field sites from recent liquefaction events (e.g. 1999 Kobe, Japan), a quality screening index for weighting the accuracy of reported case data, and a "Baysian" statistical analysis.

- The Baysian analysis performed by Cetin et al. (2004) reportedly results in empirical liquefaction relationships that have minimal bias and uncertainty as compared to the previous relationships (e.g. Youd et al., 2001).

- The liquefaction susceptibility map was developed through a five step process including:

    1. Preparation of a detailed Quaternary geological map delineating deposits age, depositional environment, and texture;
    2. Evaluation of Quaternary deposit thickness and depth to groundwater;
    3. Initial evaluation of relative liquefaction susceptibility (decision tree);
    4. Liquefaction triggering evaluation using geotechnical borehole data and the Seed and Idriss (1971b) "Simplified Procedure"; and,
    5. Identification of units of similar susceptibility and the formation of liquefaction susceptibility zones. The map depicts seven liquefaction hazard zones that range from Very Low Hazard to Very High Hazard.

- The relationship of these tasks to the development of susceptibility maps is schematically illustrated in Figure 15.7. Liquefaction susceptibility maps are constructed at a scale of 1:24,000 on these quadrangles that contain areas with conditions conducive to liquefaction.

- The methodology emphasizes the use of detailed Quaternary geologic mapping in conjunction with quantitative evaluation of subsurface information, as a basis for differentiating susceptibility classes.

- One advantage of this approach is that the categorization of borehole SPT data with respect to geologic map units allows for the extrapolation of data over areas where borehole coverage may be absent or lacking.

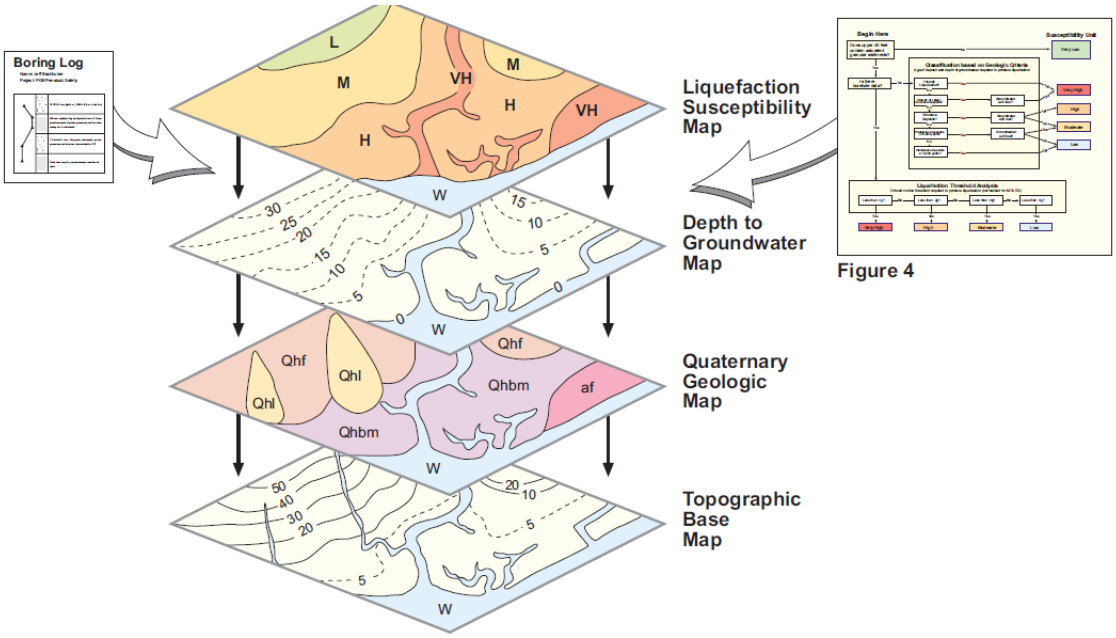

Fig 15.7: Data sources and integration procedures to produce a liquefaction susceptibility map.

- The final liquefaction susceptibility maps integrate existing subsurface data, surficial geologic mapping, and depth to groundwater to estimate triggering peak acceleration thresholds (PGA trigger).

- Seven relative susceptibility zones were established: Very High, High, Medium to High, Medium, Low to Medium, Low, and Very Low. Each of these zones has different estimated PGA liquefaction triggering levels

- In general, zones ranked as Very High and High susceptibility could potentially experience widespread and severe liquefaction under moderate to strong earthquake shaking, and possible minor to moderate liquefaction under moderate levels of earthquake shaking.

- Zones ranked as Low and Very Low susceptibility likely would either experience no significant liquefaction, or isolated and relatively minor liquefaction even under very strong earthquake shaking.

- The Medium susceptibility zones likely would experience isolated and restricted zones of severe to moderate liquefaction under strong earthquake shaking, and only very minor and sparse liquefaction under moderate levels of earthquake shaking.

- Flow chart developed in cooperation with California Geological Survey for Simi Valley, California, with ground motion thresholds required to produce liquefaction normalized for a M7.5 earthquake (from Hitchcock et al., 1999) is shwon in Figure 15.8.

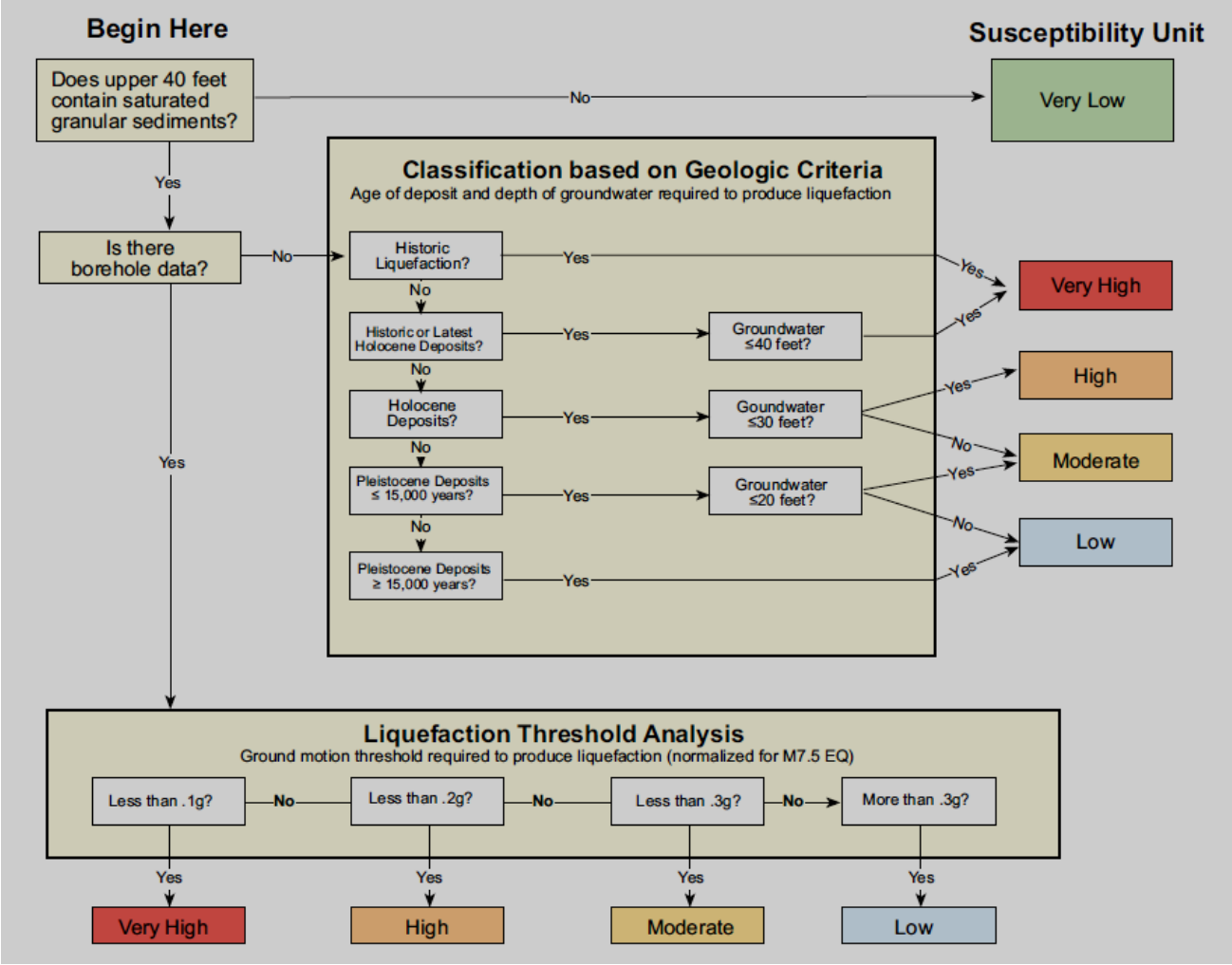

Fig 15.8: Decision flow chart for evaluation of liquefaction susceptibility. Flow chart developed in cooperation with California Geological Survey for Simi Valley, California, with ground motion thresholds required to produce liquefaction normalized for a M7.5 earthquake (from Hitchcock et al., 1999).

Topic 11

Identification factors: qualitative susceptibility to liquefaction

Table 15.2: Identification of Liquefiable Soils

Sand, muddy sand and silt	Clayey soils
S_r around 100%	$d_{15} > 5\mu$
$C_v = \frac{d_{60}}{d_{10}} < 15$	$W_L < 35\%$
$0.05 < d_{50} < 1.5$ mm	$W > 0.9\ W_L$
In the final state of the project: $\sigma'_v < 200$ kPa in zones Ia[a] and Ib[a] $\sigma'_v < 200$ kPa in zone II[a] $\sigma'_v < 300$ kPa in zone III[a]	Soil above the line 'A' of the plasticity diagram
A *contrario*, soils satisfying the following conditions can be considered to be free of liquefaction risks:	
$d_{10} > 2$mm Or $\begin{cases} d_{70} < 74\mu \\ I_p > 10\% \end{cases}$	
[a]Zones Ia, and Ib, II and III correspond to respective maximum accelerations of the order of: 1.0, 1.5, 2.5 and 3.5 m/s^2.	

- For common soils, liquefiable soils are identified by a conjunction of several criteria described, for example, in the French earthquake engineering rules, known as PS 92, in force in 1998.

Topic 12

Liquefaction susceptibility of silty and clayey sands (Andrew and Martins, 2000)

Table 15.3: Liquefaction Susceptibility of silty and clayey sands (after Andres and Martin 2000)

	Liquid Limit[a] <32%	Liquid Limit[a] ≥32%
Clay content[b] <10%	Susceptible	Further studies required (considering plastic non-clay sized grains such as mica)
Clay content[b] ≥10%	Further studies required (considering plastic non-clay sized grains such as mica and quarry tailings)	Not susceptible

[a]Liquid limit determined by Casagrande-type percussion apparatus
[b]Clay defined as grains finer than 0.002 mm

- The overburden correction factor (C_N) proposed by Liao and Whitman (1986) is preferred to normalize the SPT-N values. The estimated CRR for the soil layers with fines content more than 35% may be conservative if the procedure suggested by Youd et al. (2001) to obtain an equivalent $(N_1)_{60}$ for clean sand ($(N_1)_{60cs}$) is used.

- To overcome this limitation, the criterion given in Table above, which was suggested by Andrews and Martin (2000), is employed for the soil layers with fines content more than 35%. The soil layers with liquid limits and clay contents greater than 32% and 10%, respectively, are evaluated as non-liquefiable even if FL<1.4.

Topic 13

Cyclic Stress Ratio (CSR) and Cyclic Resistance Ratio (CRR):

- Cyclic stress ratio (CSR): As used in the original development of simplified procedure the term cyclic stress ratio refers to both the cyclic stress ratio generated by the earthquake and the cyclic stress ratio required to generate a change of state in the soil to a liquefied condition.

- Cyclic resistance ratio (CRR): The stress ratio required to cause a change of state of the soil to a liquefied condition is referred to throughout this text as the cyclic resistance ratio. This change of terminology is recommended for standard use in engineering practice in NCEER, 1997.

- Analytical Evaluation of liquefaction potential of a site is based originally on the pioneering work by Seed and Idriss (1971) The “simplified procedure” originally developed involves the calculation of the Factor of Safety obtained by determining the Cyclic Resistance Ratio and Cyclic Stress Ratio of the site soils.

- The method has been modified and improved by several researchers. The current “simplified procedure” calculates the factor of safety, FS, against liquefaction in terms of the cyclic stress ratio, CSR (the demand), and the cyclic resistance ratio, CRR (the capacity), according to the formula:

$$FS = (CRR\ 7.5/CSR).MSF.K\sigma.K\alpha \qquad (15.1)$$

- Where $CRR_{7.5}$ is the cyclic resistance ratio for magnitude 7.5 earthquakes, MSF is the Magnitude scaling factor, Kσ is the overburden correction factor, and Kα is the correction factor for sloping ground. CSR is estimated using the Seed and Idriss (1971) equation multiplied by 0.65:

$$CSR = 0.65(a/g).\sigma_{v0}/\sigma'_{v0}.rd \quad (15.2)$$

- Where a is the peak horizontal acceleration at the ground surface generated by the Earthquake, g is acceleration due to gravity, σvo and σ'vo are the total and effective overburden stresses, respectively, rd is the stress reduction coefficient and 0.65 coefficient accounts for flexibility of the soil

- Profile other than the purely empirical grain size comparisons, the three commonly used methods to evaluate the liquefaction resistance, CRR, are:
  1. Using the Standard Penetration Test (SPT),
  2. Using the Cone Penetration Test (CPT), and
  3. Using Seismic Shear wave velocity

- The seismic demand on a soil layer, expressed in terms of CSR (CSR induced by the earthquake). The cyclic stress ratio is calculated based on simplified approach recommended by Seed and Idriss (1971),

$$CSR = 0.65\left(\frac{a_{\max}}{g}\right)\left(\frac{\sigma_{v0}}{\sigma'_{v0}}\right)r_d \quad (15.3)$$

- The parameter a_{max} is the peak horizontal acceleration at the surface generated by earthquake and is calculated using relations given below.

$$M = 1 + (2/3)I_0 \quad (15.4)$$

$$Loga_{\max} = (I_0/3) - (1/2) \quad (15.5)$$

- Where I0 is the Maximum earthquake Intensity, M is the Earthquake Magnitude These two equations are proposed by Gutenberg from the earthquake data for California. The amax relation can be used for other places also. The observed N value must necessarily be corrected for overburden pressure C_N, Hammer energby C_E, Bore hole diameter C_B, Presence or absence of liner C_S, Rod length C_R, and Fine content C_{fines}. Corrected N value (N_{60}) is obtained using the following equation.

$$N_{60} = N * C_N * C_E * C_B * C_S * C_R * C_{fines} \quad (15.6)$$

Characterization of Loading

- The CSR is most commonly evaluated using the "simplified method" first described by Seed and Idriss 19721, which can be expressed as

$$CSR = 0.65\frac{a_{\max}}{g}.\frac{\sigma_{v0}}{\sigma'_{v0}}.\frac{r_d}{MSF} \quad (15.7)$$

- Where a_{max}=peak ground surface acceleration; g=acceleration of gravity in same units as a_{max}; v_o=initial vertical total stress; v_o=initial vertical effective stress; r_d=depth reduction factor; and MSF=magnitude scaling factor, which is a function of earthquake magnitude.

- The depth reduction factor accounts for compliance of a typical soil profile, and the MSF acts as a proxy for the number of significant cycles, which is related to the ground motion duration.

- It should be noted that two pieces of loading information a_{max} and earthquake magnitude are required for estimation of the CSR.

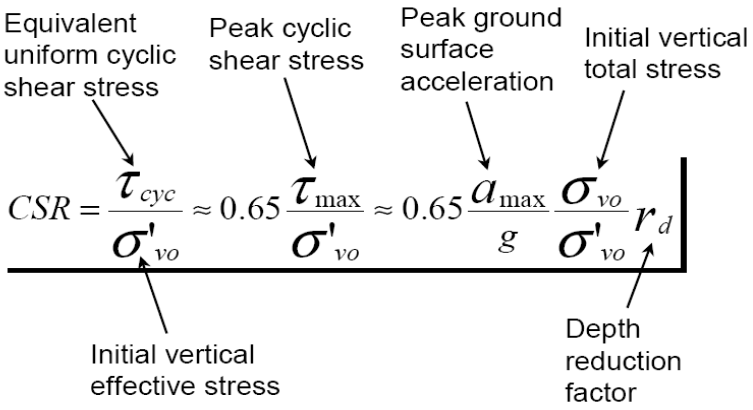

Topic 14

What procedures are preferred for estimating amax at potentially liquefiable sites

- The following three methods, in order of preference, may be used for estimating a_{max}:

1. The preferred method for estimating a_{max} at a site is through application of empirical correlations for attenuation of a_{max} as a function of earthquake magnitude, distance from the seismic energy source, and local site conditions.

   Several correlations have been developed for estimating a_{max} for sites on bedrock or stiff to moderately stiff soils. Preliminary attenuation relationships have also been developed for soft soil sites (Idriss, 1991).

   Selection of an attenuation relationship should be based on factors such as region of the country, type of faulting, site condition, etc.

2. For soft sites and other soil profiles that are not compatible with available attenuation relationships, a_{max} may be estimated from local site response analyses.

Computer programs such as SHAKE, DESRA, etc., may be used for these calculations. Input ground motions in the form of recorded accelerograms are preferable to synthetic records.

Accelerograms be used in the analysis, including as many records as feasible from earthquakes with similar magnitudes, source distances, etc.

3. The third and least desirable method for estimating peak ground acceleration is through amplification ratios, such as those developed by Idriss (1990; 1991), Seed et al.(1994), and BSSC (1994).

   These factors use a multiplier or ratio by which bedrock outcrop motions are amplified to estimate motions at ground surface. Because amplification ratios are influenced by strain level, earthquake magnitude, and perhaps frequency content, caution and considerable engineering judgment are required in the application of these relationships.

Topic 15

Which peak acceleration should be used?

1. The largest horizontal acceleration recorded on a three-component accelerogram;
2. The geometric mean (square root of the product) of the two maximum horizontal components; or
3. A vectorial combination of horizontal accelerations.

- According to I.M. Idriss (oral communication at workshop), where recorded motions were available, the larger of the two horizontal peak components of acceleration were used in the original development of the simplified procedure.

- Where recorded values were not available, which was the circumstance for most sites in the data base, peak acceleration values were estimated from attenuation relationships based on the geometric mean of the two orthogonal peak horizontal accelerations.

- In nearly all instances where recorded motions were used, the peaks from the two horizontal records were approximately equal. Thus where a single peak was used that peak and the geometric mean of the two peaks were about the same value.

- Based on this information, the workshop participants concurred that use of the geometric mean is more consistent with the derivation of the procedure and is preferred for use in engineering practice.

- However, use of the larger of the two orthogonal peak accelerations would be conservative and is allowable. Vectorial accelerations are seldom calculated and should not be used. Peak vertical accelerations are ignored for calculation of liquefaction resistance.

Topic 16

Stress Reduction Coefficient (r_d)

- r_d is the stress reduction coefficient and it accounts for flexibility of the soil profile. For routine practice and noncritical projects, the following equations 15.1 and 15.2 may be used to estimate average values of rd (Liao and Whitman 1986b):

$$r_d = 1.0 - 0.00765z \quad for \quad z \le 9.15m \tag{15.8}$$

$$r_d = 1.174 - 0.0267z \quad for \quad 9.15m < z \le 23m \tag{15.9}$$

where z = depth below ground surface in meters. Some investigators have suggested additional equations for estimating r_d at greater depths (Robertson and Wride 1998), but evaluation of liquefaction at these greater depths is beyond the depths where the simplified procedure is verified and where routine applications should be applied.

- r_d values determined from above equations are suitable for use in routine engineering practice. The user should understand, however, that there is considerable variability in the flexibility and thus r_d at field sites, that r_d calculated from above equations are the mean of a wide range of possible r_d, and that the range of r_d increases with depth (Golesorkhi 1989).

- For ease of computation, T. F. Blake (personal communication, 1996 in Youd et al., 2001) approximated the mean curve plotted in Fig. 15.9 by the following equation:

$$r_d = \frac{1.000 - 0.4113z^{0.5} + 0.04052z + 0.001753z^{1.5}}{1.000 - 0.4177z^{0.5} + 0.05729z - 0.006205z^{1.5} + 0.001210z^{2}} \tag{15.10}$$

- Where z = depth beneath ground surface in meters. Above Eq. yields essentially the same values for r_d as that of the earlier eq., but is easier to program and may be used in routine engineering practice.

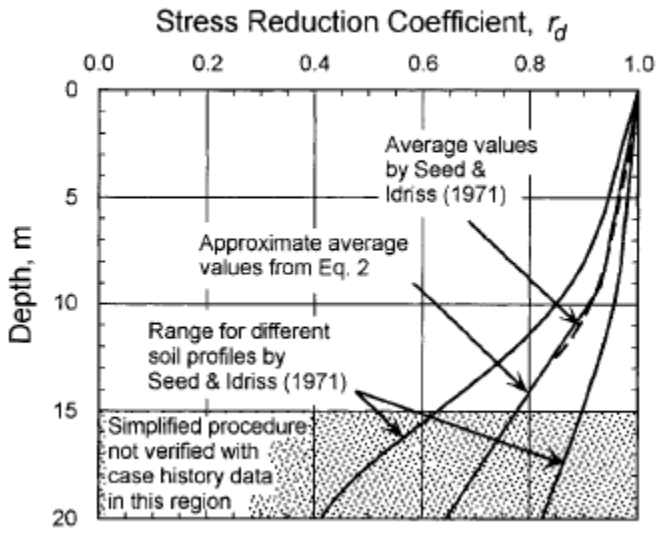

Fig 15.9: r_d versus Depth Curves Developed by Seed and Idriss (1971) with Added Mean-Value Lines Plotted from above Eq.

- Fig 15.9 r_d versus depth curves developed by Seed and Idriss (1971) with added mean value lines plotted from above Eqs.

- I. M. Idriss [Transportation Research Board (TRB) (1999)] suggested a new procedure for determining magnitude-dependent values of rd. Application of these r_d require use of a corresponding set of magnitude scaling factors that are compatible with the new r_d.

Topic 17

The capacity of the soil to resist liquefaction, expressed in terms of CRR.(CSR required to cause liquefaction)

- Many factors govern the liquefaction process for in situ soil and the most important are

1. Intensity of earthquake and its duration,
2. Location of ground water table,
3. Soil type,
4. Soil relative density,

5. Particle size gradation,
6. Particle shape,
7. Depositional environment of soil,
8. Soil drainage conditions,
9. Confining pressures,
10. Aging and cementation of the soil deposits,
11. Historical environment of the soil deposit and building/ additional loads on these deposits.

- **Earthquake intensity and duration**: In order to have liquefaction of soil, there must be ground shaking. The character of the ground motion, such as acceleration and duration of shaking, determines the shear strains that cause the contraction of the soil particles and the development of excess pore water pressures leading to liquefaction.

- **Groundwater table**: The condition most conducive to liquefaction is a near-surface groundwater table. Unsaturated soil located above the groundwater table will not liquefy.

- **Soil type**: In terms of the soil types most susceptible to liquefaction, Ishihara (1985) states: "The hazard associated with soil liquefaction during earthquakes has been known to be encountered in deposits consisting of fine to medium sand and sands containing low-plasticity fines. Occasionally, however, cases are reported where liquefaction apparently occurred in gravelly soils."

- **Soil relative density D_r**: Based on field studies, cohesionless soils in a loose relative density state are susceptible to liquefaction. Loose nonplastic soils will contract during the seismic shaking which will cause the development of excess pore water pressures.

- For dense sands, the state of initial liquefaction does not produce large deformations because of the dilation tendency of the sand upon reversal of the cyclic shear stress.

- **Particle size gradation**: Uniformly graded nonplastic soils tend to form more unstable particle arrangements and are more susceptible to liquefaction than well-graded soils. Well-graded soils will also have small particles that fill in the void spaces between the large particles. This tends to reduce the potential contraction of the soil, resulting in less excess pore water pressures being generated during the earthquake. Kramer (1996) states that field evidence indicates that most liquefaction failures have involved uniformly graded granular soils.

- **Placement conditions or depositional environment**: Hydraulic fills (fill placed under water) tend to be more susceptible to liquefaction because of the loose and segregated soil structure created by the soil particles falling through water.

Natural soil deposits formed in lakes, rivers, or the ocean also tend to form a loose and segregated soil structure and are more susceptible to liquefaction. Soils that are especially susceptible to liquefaction are formed in lacustrine, alluvial, and marine depositional environments.

- **Drainage conditions:** If the excess pore water pressure can quickly dissipate, the soil may not liquefy. Thus highly permeable gravel drains or gravel layers can reduce the liquefaction potential of adjacent soil.

- **Confining pressures**: The greater the confining pressure, the less susceptible the soil is to liquefaction. Conditions that can create a higher confining pressure are a deeper groundwater table, soil that is located at a deeper depth below ground surface, and a surcharge pressure applied at ground surface. Case studies have shown that the possible zone of liquefaction usually extends from the ground surface to a maximum depth of about 50 ft (15 m). Deeper soils generally do not liquefy because of the higher confining pressures.

- **Particle shape:** The soil particle shape can also influence liquefaction potential. For example, soils having rounded particles tend to densify more easily than angular-shape soil particles. Hence a soil containing rounded soil particles is more susceptible to liquefaction than a soil containing angular soil particles.

- **Aging and cementation**: Newly deposited soils tend to be more susceptible to liquefaction than older deposits of soil. It has been shown that the longer a soil is subjected to a confining pressure, the greater the liquefaction resistance (Ohsaki 1969, Seed 1979a, Yoshimi et al. 1989). The increase in liquefaction resistance with time could be due to the deformation or compression of soil particles into more stable arrangements. With time, there may also be the development of bonds due to cementation at particle contacts.

- **Historical environment**: It has also been determined that the historical environment of the soil can affect its liquefaction potential. For example, older soil deposits that have already been subjected to seismic shaking have an increased liquefaction resistance compared to a newly formed specimen of the same soil having an identical density (Finn et al. 1970, Seed et al. 1975).

- **Building load**: The construction of a heavy building on top of a sand deposit can decrease the liquefaction resistance of the soil. For example, suppose a mat slab at ground surface supports a heavy building. The soil underlying the mat slab will be subjected to shear stresses caused by the building load. These shear stresses induced into the soil by the building load can make the soil more susceptible to liquefaction. The reason is that a smaller additional shear stress will be required from the earthquake in order to cause contraction and hence liquefaction of the soil.

Topic 18

Evaluation of liquefaction resistance (CRR):

Laboratory tests

- **Cyclic simple shear test** - The cyclic direct simple shear test is capable of reproducing earthquake stress conditions much more accurately than is the cyclic triaxial test. It is most commonly used for liquefaction testing.

- In the cyclic direct simple shear test, a short, cyclindrical specimen is restrained against lateral expansion by rigid boundary platens, a wire-reinforced membrane, or a series of stacked rings.

- By applying cyclic horizontal shear stresses to the top or bottom of the specimen, the test specimen is deformed in much the same way as an element of soil subjected to vertically propagating s-waves

- The simple shear apparatus, however, applies shear stresses only on the top and bottom surfaces of the specimen. Since no complementary shear stresses are imposed on the vertical sides, the moment caused by the horizontal shear stresses must be balanced by non uniformly distributed shear and normal stresses (Fig 15.10).

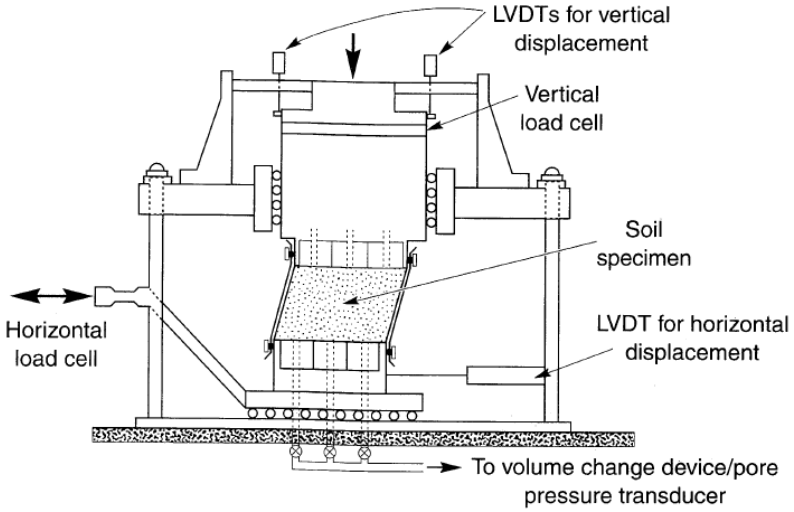

Fig 15.10: NGI cyclic simple shear apparatus. Soil Specimen is contained within wire reinforced rubber membrane (After Airey and Wood, 1987)

- **Cyclic triaxial test -** Cyclic triaxial testing has been employed to characterize liquefaction resistance of granular soils since the early 1960s. The cyclic strength curve, which graphically expresses the relationship between density, cyclic stress amplitude, and number of cycles to initiate liquefaction, is established by a series of cyclic triaxial tests where cyclic loads are applied until liquefaction occurs.

- Although liquefaction resistance determined by laboratory cyclic triaxial liquefaction tests is less valuable in engineering practice because liquefaction resistance can be altered due to sample disturbance, laboratory cyclic triaxial liquefaction tests are still useful in quantitative assessment of factors affecting liquefaction.

- Evans et al. (1994) reveals that membrane compliance affects the liquefaction resistance of uniformly graded gravels as determined by cyclic triaxial tests. Evan and Zhou (1994) conducted a series of conventional size triaxial liquefaction tests to quantify the effect of gravel content on the liquefaction resistance of sand-gravel composites.

- The results show that the increase in gravel content significantly increases the liquefaction resistance. Previous laboratory research was based on tests using conventional size (diameter 71 mm) specimens with particle size less than 10 mm. To overcome the size effect and boundaries limitation, a large-size (diameter 150 mm) cyclic triaxial apparatus had been developed.

- A plausible method for evaluating CRR is to retrieve and test undisturbed soil specimens in the laboratory. Unfortunately, in situ stress states generally cannot be reestablished in the laboratory, and specimens of granular soils retrieved with typical drilling and sampling techniques are too disturbed to yield meaningful results

- Only through specialized sampling techniques, such as ground freezing, can sufficiently undisturbed specimens be obtained. The cost of such procedures is generally prohibitive for all but the most critical projects. To avoid the difficulties associated with sampling and laboratory testing, field tests have become the state-of-practice for routine liquefaction investigations.

In-situ tests

- Several field tests have gained common usage for evaluation of liquefaction resistance, including the standard penetration test (SPT), the cone penetration test (CPT), shear-wave velocity measurements (Vs), and the Becker penetration test (BPT).

- SPTs and CPTs are generally preferred because of the more extensive databases and past experience, but the other tests may be applied at sites underlain by gravelly sediment or where access by large equipment is limited. Primary advantages and disadvantages of each test are listed in Table 15.4.

- **SPT** - Criteria for evaluation of liquefaction resistance based on the SPT have been rather robust over the years. Those criteria are largely embodied in the CSR versus $(N_1)_{60}$ plot reproduced in Fig. 15.11.

- $(N_1)_{60}$ is the SPT blow count normalized to an overburden pressure of approximately 100 kPa (1 ton/sq ft) and a hammer energy ratio or hammer efficiency of 60%. The normalization factors for these corrections are discussed in the section entitled Other Corrections.

Feature	Test Type			
	SPT	CPT	Vs	BPT
Past measurements at liquefaction sites	Abundant	Abundant	Limited	Sparse
Type of stress-strain behavior influencing test	Partially drained, large strain	Drained, large strain	Small strain	Partially drained, large strain
Quality control and repeatability	Poor to good	Very good	Good	Poor

Table 15.4: Comparison of Advantages and Disadvantages of Various Field Tests for Assessment of Liquefaction Resistance

Detection of variability of soil deposits	Good for closely spaced tests	Very good	Fair	Fair
Soil types in which test is recommended	Nongravel	Nongravel	All	Primarily gravel
Soil sample retrieved	Yes	No	No	No
Test measures index or engineering property	Index	Index	Engineering	Index

- Fig. 15.11 is a graph of calculated CSR and corresponding $(N_1)_{60}$ data from sites where liquefaction effects were or were not observed following past earthquakes with magnitudes of approximately 7.5. CRR curves on this graph were conservatively positioned to separate regions with data indicative of liquefaction from regions with data indicative of nonliquefaction.

- Curves were developed for granular soils with the fines contents of 5% or less, 15%, and 35% as shown on the plot. The CRR curve for fines contents <5% is the basic penetration criterion for the simplified procedure and is referred to hereafter as the ‘‘SPT cleansand base curve.’’ The CRR curves in Fig. are valid only for magnitude 7.5 earthquakes.

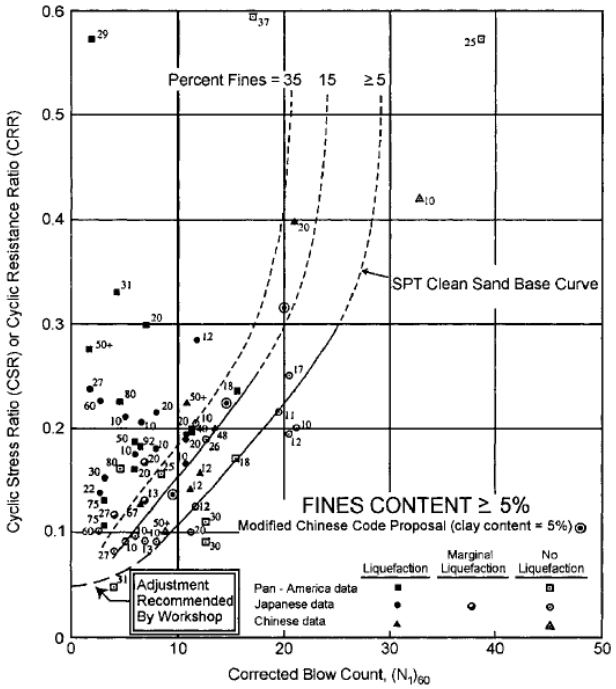

Fig 15.11: SPT Clean-Sand Base Curve for Magnitude 7.5 Earthquakes with Data from Liquefaction Case Histories (Modified from Seed et al. 1985)

- **CPT** - A primary advantage of the CPT is that a nearly continuous profile of penetration resistance is developed for stratigraphic interpretation. The CPT results are generally more consistent and repeatable than results from other penetration tests.

- The continuous profile also allows a more detailed definition of soil layers than the other tools listed in the table. This stratigraphic capability makes the CPT particularly advantageous for developing liquefaction-resistance profiles. Interpretations based on the CPT, however, must be verified with a few well-placed boreholes preferably with standard penetration tests, to confirm soil types and further verify liquefaction resistance interpretations.

- Fig 15.12. Provides curves prepared by Robertson and Wride (1998) for direct determination of CRR for clean sands (FC $\leq$ 5%) from CPT data. This figure was developed from CPT case history data compiled from several investigations, including those by Stark and Olson (1995) and Suzuki et al. (1995).

- The chart, valid for magnitude 7.5 earthquakes only, shows calculated cyclic resistance ratio plotted as a function of dimensionless, corrected, and normalized CPT resistance qc_{1N} from sites where surface effects of liquefaction were or were not observed following past earthquakes.

- The CRR curve conservatively separates regions of the plot with data indicative of liquefaction from regions indicative of nonliquefaction.

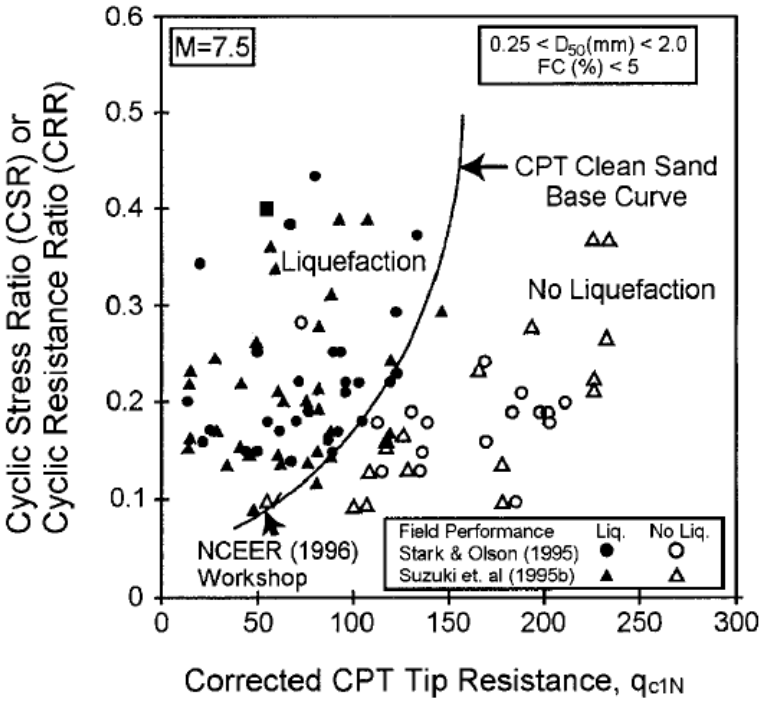

Fig 15.12: Curve Recommended for Calculation of CRR from CPT Data along with Empirical Liquefaction Data from Compiled Case Histories (Reproduced from Robertson and Wride 1998)

- **Vs -** Andrus and Stokoe (1997, 2000) developed liquefaction resistance criteria from field measurements of shear wave velocity Vs. The use of Vs as a field index of liquefaction resistance is soundly based because both Vs and CRR are similarly, but not proportionally, influenced by void ratio, effective confining stresses, stress history, and geologic age.

- The advantages of using Vs include the following:

    1. Vs measurements are possible in soils that are difficult to penetrate with CPT and SPT or to extract undisturbed samples, such as gravelly soils, and at sites where borings or soundings may not be permitted;
    2. Vs is a basic mechanical property of soil materials, directly related to small-strain shear modulus; and
    3. The small-strain shear modulus is a parameter required in analytical procedures for estimating dynamic soil response and soil structure interaction analyses.

- Three concerns arise when using Vs for liquefaction-resistance evaluations:
    1. Seismic wave velocity measurements are made at small strains, whereas pore-water pressure buildup and the onset of liquefaction are medium- to high-strain phenomena;
    2. Seismic testing does not provide samples for classification of soils and identification of nonliquefiable soft clay-rich soils; and
    3. Thin, low Vs strata may not be detected if the measurement interval is too large.

- Therefore the preferred practice is to drill sufficient boreholes and conduct in situ tests to detect and delineate thin liquefiable strata, nonliquefiable clay-rich soils, and silty soils above the ground-water table that might become liquefiable should the water table rise.

- Other tests, such as the SPT or CPT, are needed to detect liquefiable weakly cemented soils that may have high Vs values.

- **BPT** - Liquefaction resistance of nongravelly soils has been evaluated primarily through CPT and SPT, with occasional Vs measurements. CPT and SPT measurements, however, are not generally reliable in gravelly soils.

- Large gravel particles may interfere with the normal deformation of soil materials around the penetrometer and misleadingly increase penetration resistance. Several investigators have employed large-diameter penetrometers to surmount these difficulties; the Becker penetration test (BPT) in particular has become one of the more effectively and widely used larger tools.

- The BPT was developed in Canada in the late 1950s and consists of a 168-mm diameter, 3-m-long double-walled casing driven into the ground with a double-acting diesel-driven pile hammer.

- The hammer impacts are applied at the top of the casing and peneration is continuous. The Becker penetration resistance is defined as the number of blows required to drive the casing through an increment of 300 mm.

- The BPT has not been standardized, and several different types of equipment and procedures have been used. There are currently very few liquefaction sites from which BPT data have been obtained.

- Thus the BPT cannot be directly correlated with field behavior, but rather through estimating equivalent SPT N-values from BPT data and then applying evaluation procedures based on the SPT. This indirect method introduces substantial additional uncertainty into the calculated CRR.

Topic 19

SPT -Based Procedure for Evaluating Liquefaction Potential and Remarks on CRR from SPT

- Semi-empirical procedures for liquefaction evaluations originally were developed using the Standard Penetration Test (SPT), beginning with efforts in Japan to differentiate between liquefiable and nonliquefiable conditions in the 1964 Niigata earthquake (e.g., Kishida 1966).

- Subsequent developments have included contributions from many researchers, especially in the investigations of individual case histories. The procedures recommended by Seed et al (1984, 1985) to obtain and adjust the SPT blow count and to obtain the values of CRR are particularly note worthy as they have set the standard for almost two decades of subsequent engineering practice.

- The NCEER/NSF workshop in 1996/98 resulted in a number of suggested revisions to the SPT-based procedure but with only minor adjustments to the CRR – $(N_1)_{60}$ curve for clean sands put forth by Seed et al (1984).

- Cetin et al (2000) reexamined and expanded the SPT case history database. The data set by Seed et al (1984) had some 125 cases of liquefaction/no-liquefaction in 19 earthquakes, of which 65 cases pertain to sands with fines content FC ≤ 5%, 46 cases had 6% ≤ FC ≤ 34%, and 14 cases had FC ≥ 35%.

- Cetin et al (2000) included an additional 67 cases of liquefaction/no-liquefaction in 12 earthquakes, of which 23 cases pertain to sands with FC ≤ 5%, 32 cases had 6% ≤ FC ≤ 34%, and 12 cases had FC ≥ 35%.

- Cetin et al (2000) used their expanded data set and site response calculations for estimating CSR to develop revised deterministic and probabilistic liquefaction relationships. The results of Cetin et al (2000) were also summarized in Seed et al (2001).

- The revaluation of the SPT-based procedures that is presented herein incorporates several different adjustments and parameter revisions. The CSR and $(N_1)_{60}$ values were recalculated using the revised r_d, MSF, $K\sigma$, and C_N relations recommended herein.

- The C_N and $K\sigma$ relations for silty sands were computed using the equivalent clean sand $(N_1)_{60}$ values, which appears to be a reasonable approximation pending better experimental definition of how fines content affects these relations.

- For case histories where strong motion recordings showed that liquefaction occurred early in shaking, CSR were adjusted to reflect the number of equivalent cycles that had occurred up to the time when liquefaction was triggered (Idriss 2002).

- Experimental data and theoretical considerations that provide guidance on the shape of the CRR – $(N_1)_{60}$ curve at high $(N_1)_{60}$ values (where there is very limited case history data) were re-examined.

- In particular, the SPT and CPT correlations were developed in parallel to maintain consistency between the two procedures. A few additional comments on some of these aspects are provided below.

- The revised r_d relation was used to estimate CSR for each case history, as opposed to using site response studies. The main reason is that, except for a few cases, the available information for the liquefaction/no-liquefaction case histories is insufficient to have confidence that detailed site response analyses would be more accurate.

- The $K\sigma$ factor is normally applied to the "capacity" side of the analysis during design, but it must also be used to convert the site CSR to a common σ 'vo value for the empirical derivation of a CRR – $(N_1)_{60}$ curve. This is accomplished as:

$$(CSR)_{M-7.5} = 0.65\left(\frac{\sigma_{v0} a_{\max}}{\sigma'_{v0}}\right)\frac{r_d}{MSF}\frac{1}{K_\sigma} \qquad (15.11)$$

- Such that the values of CSR correspond to an equivalent σ 'vo of 1 atm, and thus the liquefaction correlation also corresponds to an equivalent σ 'vo of 1 atm. Since Kσ has been restricted to ≤1, this only affects a few of the case history points. Note that in applying the liquefaction correlation in design, the Kσ factor is still applied to the capacity.

- The shape of the CRR – $(N_1)_{60}$ curve at the higher range of $(N_1)_{60}$ values is guided by experimental and theoretical considerations because there is insufficient case history data to constrain the curve in this range.

- In 1982, Seed and Idriss set the CRR – $(N_1)_{60}$ curve asymptotic to vertical at $(N_1)_{60} \approx 35$ because the shake table results of De Alba et al (1976) indicated that the slope of the CRR - D_R relation would increase substantially at high values of D_R .

- Seed et al (1984) similarly kept the CRR – $(N_1)_{60}$ curve asymptotic to vertical, but at $(N_1)_{60} \approx 30$. In the work presented herein, the CRR – $(N_1)_{60}$ relation was assigned a very steep, but non-vertical, slope based on a revaluation of experimental results for high quality field samples obtained by frozen sampling techniques (e.g., Yoshimi et al 1984, 1989) and judgments based on theoretical considerations.
- In this regard, the application of probabilistic methods to the development of liquefaction correlations has often suffered from not including experimental and theoretical constraints on the liquefaction correlations at high CRR and $(N_1)_{60}$ values.

- Consequently, such probabilistic methods often predict probabilities of liquefaction at high $(N_1)_{60}$ values that are unreasonably high. It is believed that including experimental and theoretical findings in the development of probabilistic relations would improve the results in the upper range of CRR and $(N_1)_{60}$ values.

- The SPT and CPT data were utilized together in developing a consistent pair of liquefaction correlations for the cases with FC ≤ 5%. The consistency between the two in-situ test types was achieved through a common CRR - ζ_R relation (Boulanger and Idriss 2004) as opposed to a constant q_{CN} / N_{60} ratio as had been used in some past studies.

- Maintaining a common CRR - ζ_R relation results in a q_{CN} / N_{60} ratio that is dependent on DR . The corresponding $q_{C1N} / (N_1)_{60}$ ratio (in lieu of q_{CN} / N_{60} ratio) can be determined to obtain:

$$\frac{q_{C1N}}{(N_1)_{60}} = \frac{(2.092 D_R + 2.224)^{3.788}}{46(D_R)^2} \qquad (15.12)$$

- The $q_{C1N} / (N_1)_{60}$ ratios are plotted versus $(N_1)_{60}$ in Figure below, which shows values that range from greater than 10 in very loose sands to about 5.5 in very dense sands.

- In the range of particular interest, which is approximately $10 \leq (N_1)_{60} \leq 25$, the calculated $q_{C1N} / (N_1)_{60}$ ratio ranges from 6 to 8.

- The variation of the $q_{C1N} / (N_1)_{60}$ ratio with D_R is consistent with the expected differences in drainage conditions for these two in situ tests. The CPT is a quasistatic test that is largely drained or partially drained, depending on the grain size distribution of the cohesionless soils, whereas the SPT is a dynamic test that is largely undrained.

- Thus, it would be expected that for SPT tests, loose sand would develop positive excess pore pressures while dense sand would more likely develop negative excess pore pressures. This difference in drainage conditions can explain, at least in part, the trend depicted in Figure 15.13.

- Revised CRR – $(N_1)_{60}$ relations, derived incorporating the above considerations, are presented in Figures 15.14 and 15.15. The cases for cohesionless soils having FC $\leq$ 5% are plotted in Figure 15.14 along with the curve agreed to at the NCEER/NSF workshop.

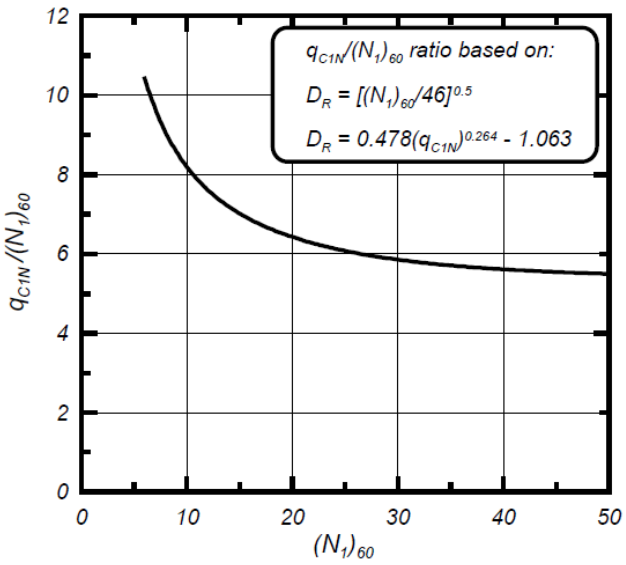

Fig 15.13: Ratio of CPT and SPT penetration resistances based on adopted correlations to relative density.

- Also shown in Figure 15.14 and 15.15 below is the new curve proposed herein. The individual cases are those from Seed et al (1984) and Cetin et al (2000) subject to the previously described adjustments. The proposed changes to the CRR – $(N_1)_{60}$ relation are relatively modest.

- For $(N_1)_{60}$ values between 8 and 25, the maximum difference in CRR is about 15% at $(N_1)_{60}$ ≈20. The revised relation for FC ≤ 5% is further compared to other published relations in Figure 15.14, including relations from early in their development (i.e., Seed 1979) to a very recent relation by Cetin et al (2000) that is summarized in Seed et al (2001).
-
- Note that the curves and the data points for the liquefaction/no-liquefaction case histories pertain to magnitude M = 7½ earthquakes and an effective vertical stress σ 'vo = 1 atm (≈ 1 tsf).

- The cases for cohesionless soils with FC ≥ 35% are plotted in Figure 15.16 along with the applicable curve agreed to at the NCEER/NSF workshop and the new curve proposed herein. Several case history points fall well below the FC ≥ 35% boundary curve agreed to at the NCEER/NSF workshop and these points control the position of the revised curve.

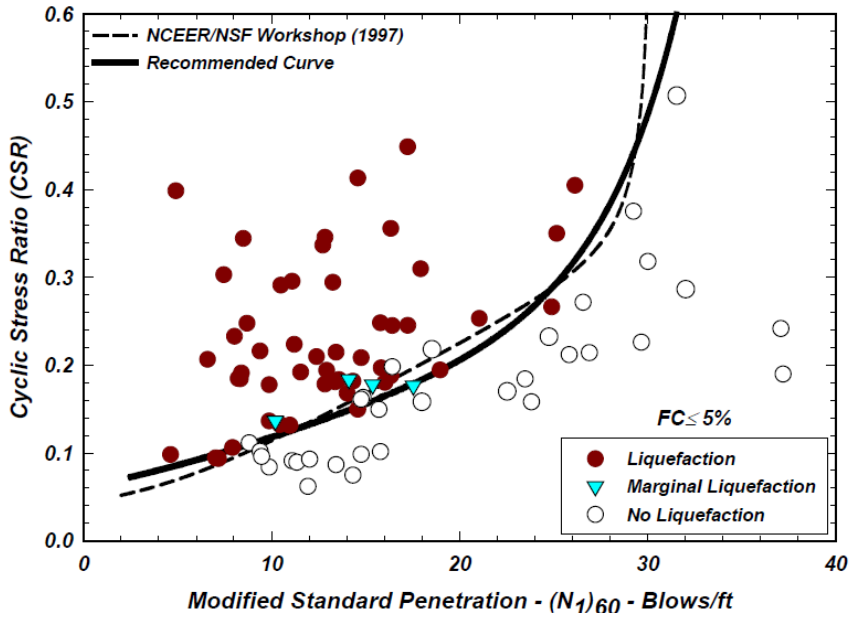

Fig 15.14: SPT case histories of clean sands with the curve proposed by the NCEER Workshop (1997) and the recommended curve for M = 7½ and σ 'vo = 1 atm (≈1 tsf).

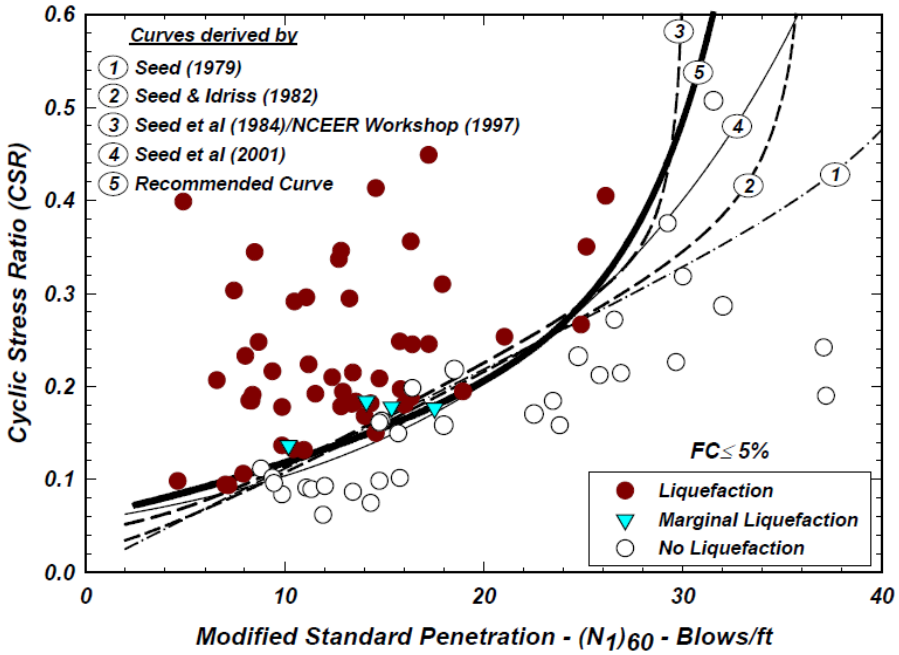

Fig 15.15: Curves relating CRR to $(N_1)_{60}$ published over the past 24 years for clean sands and the recommended curve for M = 7½ and σ 'vo = 1 atm (≈1 tsf).

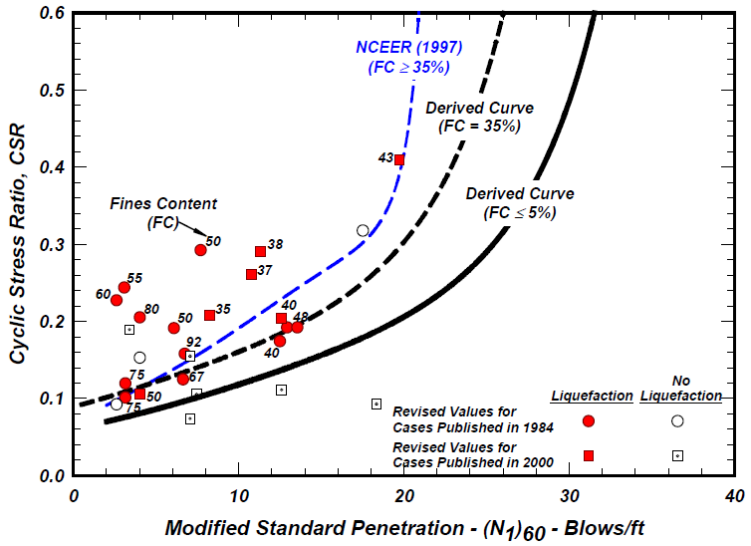

Fig 15.16: SPT case histories of cohesionless soils with FC ≥ 35% and the NCEER Workshop (1997) curve and the recommended curves for both clean sand and for FC = 35% for M = 7½ and σ 'vo = 1 atm (≈ 1 tsf).

- The FC =15% boundary curve that was recommended at the NCEER/NSF workshop and the revised FC =15% boundary curve proposed herein are compared in Figures 15.17

- Figure 15.17a shows the case history points for cohesionless soils with 5%< FC <15%, while Figure 15.17b shows the cases for 15%≤FC <35%. The revised curve is lower than the curve recommended at the NCEER/NSF workshop, reflecting the influence of the revised case history data set compiled by Cetin et al (2000).

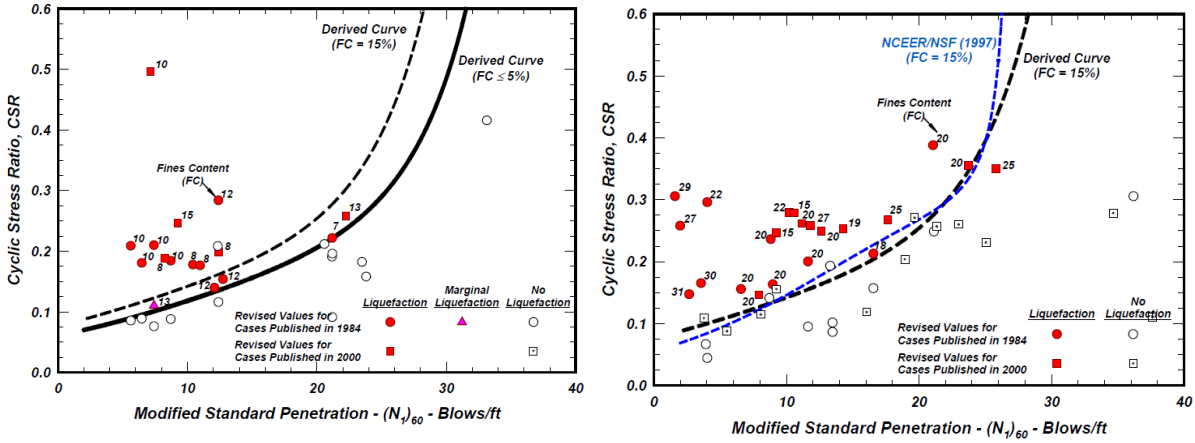

a **b**

Fig 15.17: SPT case histories of cohesionless soils with (a) 5%< FC <15% and the recommended curves for both clean sands and for FC =15% for M = 7½ and σ 'vo = 1 atm (≈ 1 tsf) (b) 15%≤ FC <35% and the NCEER Workshop (1997) curve and the recommended curve for FC =15% for M = 7½ and σ 'vo = 1 atm (≈ 1 tsf).

- The revised boundary curves proposed herein for cohesionless soils can be expressed using the following equations. First, the SPT penetration resistance is adjusted to an equivalent clean sand value as:

$$(N_1)_{60cs} = (N_1)_{60} + \Delta(N_1)_{60} \qquad (15.13)$$

$$(N_1)_{60} = \exp\left(1.63 + \frac{9.7}{FC} - \left(\frac{15.7}{FC}\right)^2\right) \qquad (15.14)$$

- The variation of $\Delta(N_1)_{60}$ with FC , calculated using the above equation, is presented in Figure 15.18. The value of CRR for a magnitude M =7½ earthquake and an effective vertical stress σ 'vo =1 atm (≈ 1 tsf) can be calculated based on $(N_1)_{60cs}$ using the following expression:

$$CRR = \exp\left\{\frac{(N_1)_{60cs}}{14.1} + \left(\frac{(N_1)_{60cs}}{126}\right)^2 - \left(\frac{(N_1)_{60cs}}{23.6}\right)^3 + \left(\frac{(N_1)_{60cs}}{25.4}\right)^4 \right. \qquad (15.15)$$

- The use of these equations provides a convenient means for evaluating the cyclic stress ratio required to cause liquefaction for a cohesionless soils with any fines content.

- Additional research is needed to develop guidelines for evaluating the combined effects of fines content and fines plasticity on the behavior of sands. In the absence of adequate data on this issue, it is suggested that cohesionless soil behavior would include soils whose fines fraction has a plasticity index (PI) less than about 5±.

- It must be stressed that the quality of the site characterization work is extremely important for the reliable evaluation of liquefaction potential. With regard to SPT testing, it is vital that the testing procedures carefully adhere to established standards (as summarized at the NCEER Workshop 1997) and that, regardless of the test procedures, SPT tests can produce misleading $(N_1)_{60}$ values near contacts between soils of greatly differing penetration resistances (e.g., sand overlying soft clay) and can miss relatively thin critical strata.

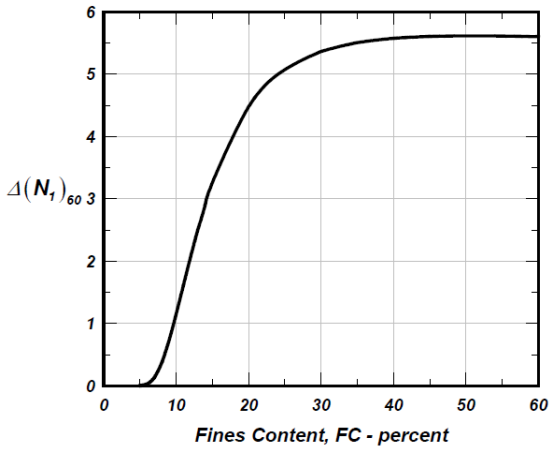

Fig 15.18: Variation of $\Delta(N_1)_{60}$ with fines content.

- Such difficulties have been reported in many cases (e.g., Boulanger et al 1995, 1997) and are generally recognized as requiring careful diligence in the field investigations. In this regard, companion CPT soundings are extremely valuable, whenever possible, for identifying SPT $(N_1)_{60}$ values that might have been adversely affected by overlying or underlying strata, and for enabling a more reliable characterization of thin liquefiable strata (e.g., Robertson and Wride 1997, Moss 2003).

Topic 20

CPT -Based Procedure for Evaluating Liquefaction Potential and Comments Regarding the CPT-Based Procedure

- The Cone Penetration Test (CPT) has proven to be a valuable tool in characterizing subsurface conditions and in assessing various soil properties, including estimating the potential for liquefaction at a particular site.

- The main advantages of using the CPT are that it provides a continuous record of the penetration resistance and is less vulnerable to operator error than is the SPT test, whereas its main disadvantage is the unavailability of a sample.
- Zhou (1980) used observations from the 1978 Tangshan earthquake to propose the first liquefaction correlation based directly on CPT case histories. Seed and Idriss (1981) as well as Douglas et al (1981) proposed the use of correlations between the SPT and CPT to convert the then available SPT-based charts for use with the CPT.

- In recent years, the expanding data-base for field case histories has produced several CPT-based correlations (e.g., Shibata and Teparaksa 1988; Stark and Olson 1995; Suzuki et al 1995, 1997; Robertson and Wride 1997; Olsen 1997; Moss 2003; Seed et al 2003).

- The CPT-based liquefaction correlation was reevaluated by Idriss and Boulanger (2003) using case history data compiled by Shibata and Teparaksa (1988), Kayen et al (1992), Boulanger et al (1995, 1997), Stark and Olson (1995), Suzuki et al (1997), and Moss (2003).

- The work of Moss (2003) was particularly valuable in providing the most comprehensive compilation of field data and associated interpretations. This re-evaluation of the CPT-based procedures incorporated adjustments and parameter revisions that are similar to those previously described for the SPT reevaluation.

- For case histories where strong motion recordings showed that liquefaction occurred early in shaking, CSR were adjusted to reflect the number of equivalent cycles that had occurred up to the time when liquefaction was triggered. All CSR and q_{C1N} values were recalculated using the revised rd , MSF , $K\sigma$, and C_N relations summarized above.

- The shape of the CRR – q_{C1N} curve at high q_{C1N} values was re-examined, and the CPT and SPT correlations were developed in parallel to maintain consistency between these procedures.

- The revised CRR – q_{C1N} relation, derived using the above considerations, is shown in Figure below with the case history points for cohesionless soils having FC ≤ 5%.

- The derived relation can be conveniently expressed as:

$$CRR = \exp\left\{\frac{q_{C1N}}{540} + \left(\frac{q_{C1N}}{67}\right)^2 - \left(\frac{q_{C1N}}{80}\right)^3 + \left(\frac{q_{C1N}}{114}\right)^4 - 3\right. \qquad (15.16)$$

- This CRR – q_{C1N} relation is compared in Figure 15.19 to those by Shibata and Teparaksa (1988), Robertson and Wride (1997), Suzuki et al (1997), and the 5% probability curve by Moss (2003) as summarized in Seed et al 2003.

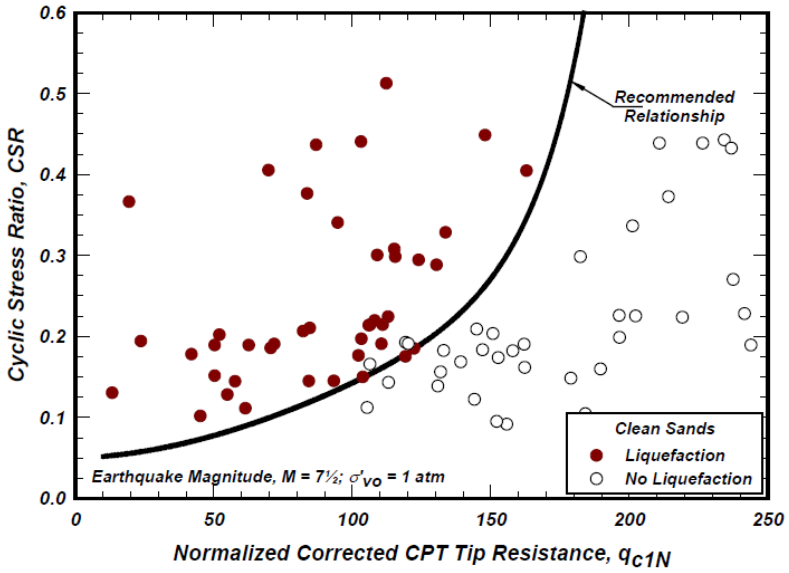

Fig 15.19: CPT-based case histories and recommended relation for clean sands for M = 7½ and σ 'vo = 1 atm (≈1 tsf).

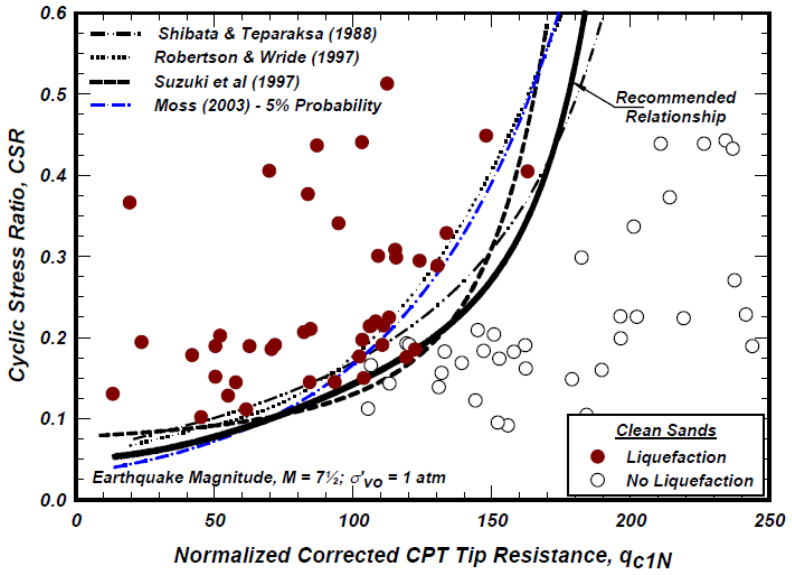

Fig 15.20: CPT-based case histories and recommended relation for clean sands with relations proposed by others.

- The derived relation is comparable to the curve proposed by Suzuki et al (1997) for clean sands. It is more conservative than the corresponding curves by Robertson and Wride (1997) and by Seed et al (2003) for almost the entire range of q_{C1N} .

- The curve proposed by Shibata and Teparaksa (1988) is less conservative than the derived relation except for q_{C1N} greater than about 165. Note that these relations and the plotted data pertain to magnitude M =7½ earthquakes and an effective vertical stress σ 'vo =1 atm (≈1 tsf).

- As previously mentioned, the CPT and SPT liquefaction correlations were developed in parallel to maintain consistency in terms of their implied CRR – ζ_R relations for clean cohesionless soils.

- Following this approach, the CRR – ζ_R relations produced for the SPT and CPT liquefaction correlations are compared in Figure below. As intended, the two relations are basically identical.

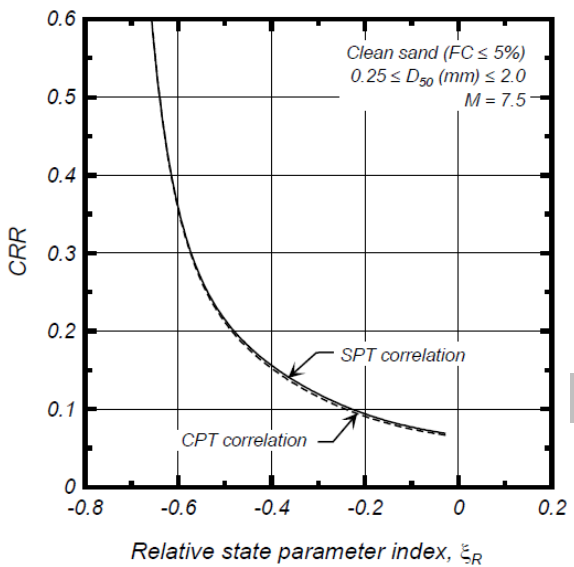

Fig 15.21: Field CRR - ζ_R relations derived from liquefaction correlations for SPT and CPT.

- The effect of fines content on the CRR – q_{C1N} relation is still being re-evaluated. This issue includes the actual effect of fines content and the most reliable means of incorporating this effect into CPT-based procedures.

- While revised procedures are not provided herein, a few comments regarding this issue are warranted. Robertson and Wride (1997) and Suzuki et al (1997) suggested the use of the "soil behavior type index", Ic (Jefferies and Davies 1993), which is a function of the tip resistance (q_C) and sleeve friction ratio (R_f), to estimate the values of CRR for cohesionless soils with high fines content.

- The curve recommended by Robertson and Wride (1997) relating CRR - q_{C1N} at Ic =2.59 (defined by Robertson and Wride as corresponding to an "apparent" fines content FC =35%) is presented in below Figure. Also shown in this figure are the CPT-based data points for the cases examined by Moss (2003) for cohesionless soils with FC ≥35%. As can be seen in the figure, the curve recommended by Robertson and Wride (1997) is unconservative.

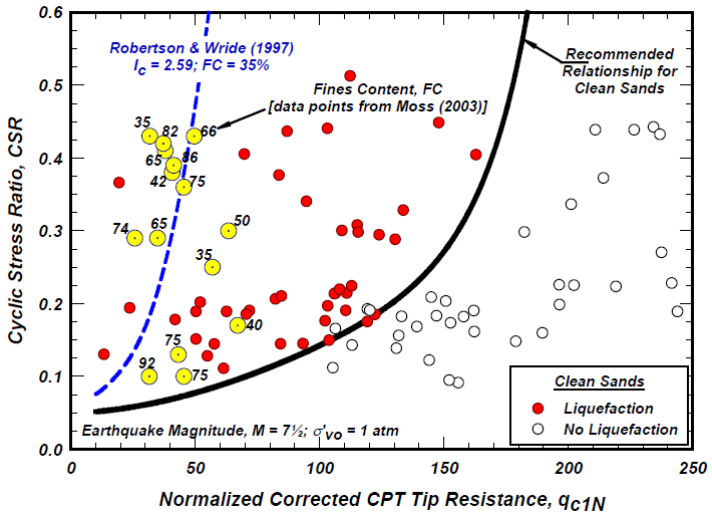

Fig 15.22: Comparison of field case histories for cohesionless soils with high fines content and curve proposed by Robertson & Wride (1997) for soils with Ic = 2.59 (apparent FC = 35%)

- Similarly, the relations by Suzuki et al (1997) for cohesionless soils with high fines content are unconservative. The recent work by Moss (2003) using friction ratio R_f in lieu of the parameter Ic as a proxy for fines content appears promising, but does require further scrutiny before it is adopted.

- Direct soil sampling should always be the primary means for determining grain characteristics for the purpose of liquefaction evaluations. The use of CPT data alone for determining grain characteristics can lead to unreliable results in many cases, particularly when dealing with soils in the transitional range between silty sand and silty clay.

- Automated analysis procedures for liquefaction evaluations using CPT data must be carefully checked for potentially misleading results near contacts between soils of greatly different penetration resistances and in finely inter-layered soils.

- Measurements of q_C and R_f near such contacts are not representative of the actual soil conditions, and the point-by-point liquefaction analysis of such data is more likely to produce meaningless results than not.

- The various difficulties that can be encountered using CPT-only procedures, and the steps needed to avoid these difficulties, were illustrated by Boulanger et al (1999) and Kulasingam et al (1999) in their analyses of the CPT soundings that were adjacent to the slope inclinometers at Moss Landing in the 1989 Loma Prieta earthquake.

- The three slope inclinometers were located at different positions along a sloping shoreline that spread laterally toward the adjacent channel. The displacement profiles from the inclinometers identify the intervals over which significant shear strains, and hence liquefaction, appear to have developed.

- Subsequent comparisons of predicted and observed soil displacement profiles provided clear examples of the types of difficulties/limitations that can be encountered with automated CPT-only analysis procedures. Fortunately, many of the common errors can be avoided by explicit consideration of soil sample data and site stratigraphy.

Topic 21

Vs Criteria for Evaluating Liquefaction Resistance and Comments Regarding the Vs-Based Procedure

- The shear wave velocity (Vs) based procedure has advanced significantly in recent years, with improved correlations and more complete databases, as recently summarized by Andrus and Stokoe (2000) and Andrus et al (2003).

- This procedure can be particularly useful for sites underlain by difficult to penetrate or sample soils (e.g., gravels, cobbles, boulders). As such, Vs –based correlations provide a valuable tool that ideally is used in conjunction with SPT- or CPT-based liquefaction correlations if possible.

- The question that arises, however, is which methodology should be given greater weight when parallel analyses by SPT, CPT, and/or Vs procedures produce contradictory results. SPT, CPT, and Vs measurements each have their particular advantages and disadvantages for liquefaction evaluations, but a particularly important point to consider is their respective sensitivity to the relative density, DR , of the cohesionless soil under consideration.

- For example, changing the D_R of a clean sand from 30% to 80% would be expected to increase the SPT blow count by a factor of about 7.1 and the CPT tip resistance by a factor of about 3.

- In contrast, the same change in D_R would be expected to only change the Vs by a factor of roughly 1.4 based on available correlations. For example, Seed and Idriss (1970) suggested the parameter K_2 max would be 34 and 64 for D_R of 30% and 80%, respectively, which give Vs values that vary by a factor of $\sqrt{(64 / 34)}= 1.37$.

- It is likely that this range will be somewhat larger for gravelly soils. Given that D_R is known to have a strong effect on the cyclic and post-cyclic loading behavior of saturated sand, it appears that Vs measurements would be the least sensitive for distinguishing among different types of behavior.

- For this reason, it may be more appropriate to view the Vs case history data-base as providing bounds that identify conditions where liquefaction is potentially highly likely, conditions where liquefaction is potentially highly unlikely, and conditions where it is uncertain whether or not liquefaction should be expected.

- As such, there continues to be a need for an improved understanding of Vs -based correlations and an assessment of their accuracy relative to SPT- and CPT-based correlations. In the mean time, it is recommended that greater weight be given to the results of SPT- or CPTbased liquefaction evaluations for materials without large particle sizes.

Topic 22

Dilatometer Test (DMT)-Based Procedure for Evaluating Liquefaction Potential

- Marchetti (1982) and later studies (Robertson and Campanella 1986, Reyna and Chameau 1991) suggested that the horizontal stress index K_D from DMT ($K_D = (p_0 - u_0) / \sigma'_{v0}$) is a suitable index parameter of liquefaction resistance.

- Comparative studies have indicated that K_D is noticeably reactive to stress history, prestraining/aging, cementation, structure – all factors increasing liquefaction resistance (scarcely felt by qc from CPT, see e.g. Huang and Ma 1994, and in general by cylindricalconical probes).

- As noted by Robertson and Campanella (1986), it is not possible to separate the individual contribution of each factor on K_D. On the other hand, a low K_D signals that none of the above factors is high, i.e. the sand is loose, uncemented, in a low K_0 environment and has little stress history.

- A sand under these conditions may liquefy or develop large strains under cyclic loading. The most significant findings supporting a well-based CRR-K_D correlation (Monaco et al. 2005) are:

- **Sensitivity of DMT in monitoring soil densification:** The high sensitivity of the DMT in monitoring densification, demonstrated by several studies (e.g. Schmertmann et al. 1986 and Jendeby 1992 found DMT ≈ twice more sensitive than CPT), suggests that the DMT may also sense sand liquefiability. A liquefiable sand may be regarded as a "negatively compacted" sand, plausibly the DMT sensitivity holds both in the positive and the negative range.

- **Sensitivity of DMT to prestraining:** CC research by Jamiolkowski and Lo Presti (1998) has shown that K_D is much more sensitive to cyclic prestraining – one of the most difficult effects to detect by any method – than penetration resistance. Given the strong link of prestraining with aging, this point is discussed in more detail in the Section "Sensitivity of K_D to aging".

- **Correlation K_D - Relative density:** The correlation by Reyna and Chameau (1991) for deriving the relative density D_R from K_D in N_C uncemented sands (Figure 15.23 (a)) has been strongly confirmed by subsequent research, in particular by additional K_D -D_R datapoints (shaded areas in Figure 15.23 (a)) obtained by Tanaka and Tanaka (1998) at the sites of Ohgishima and Kemigawa, where D_R was determined on high quality frozen samples.

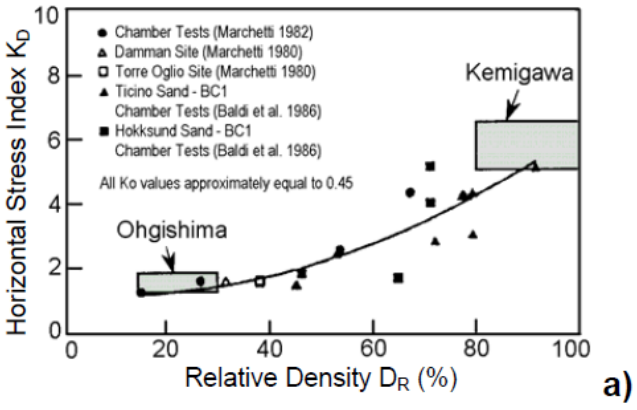

a)

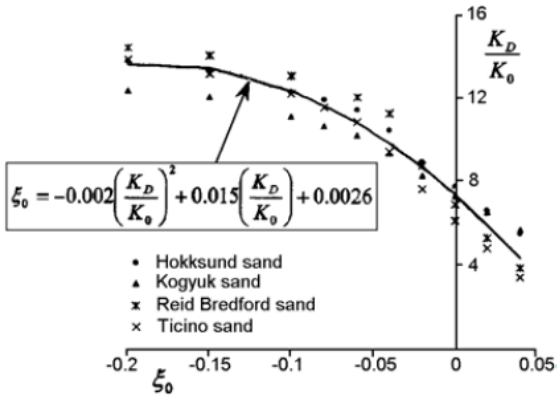

b)

Fig 15.23: (a) Correlation K_D -D_R for N_C uncemented sands (Reyna and Chameau 1991), also including Ohgishima and Kemigawa datapoints obtained by Tanaka and Tanaka (1998) on high quality frozen samples. (b) Average correlation K_D - in situ state parameter ξ_0 (Yu 2004).

- **Correlation K_D - In situ state parameter:** The state parameter concept is an important step forward in characterizing soil behaviour, combining the effects of both relative density and stress level in a rational way. The state parameter (vertical distance between current state and critical state line in the usual e - ln p' plot) governs the tendency of a sand to increase or decrease in volume when sheared, hence it is strongly related to liquefaction resistance.

- More rational methods for evaluating CRR would require the use of the state parameter (e.g. Boulanger 2003, Boulanger and Idriss 2004). Recent research supports viewing K_D from DMT as an index reflecting the in situ state parameter $\xi 0$. Yu (2004) identified the average correlation K_D - ξ_0 shown in Figure 15.23 (b) (study on four well-known reference sands). Relations K_D - ξ_0 as the one shown by Yu (2004) strongly encourage efforts to develop methods to assess liquefiability by DMT.

- **Physical meaning of K_D:** Despite the complexity of the phenomena involved in the blade penetration, the reaction of the soil against the blade could be seen as an indicator of the soil reluctance to a volume reduction. Clearly a loose collapsible soil will not strongly contrast a volume reduction and will oppose a low $\sigma'h$ (hence a low K_D) to the blade insertion. Moreover such reluctance is determined at existing ambient stresses increasing with depth (apart an alteration of the stress pattern in the vicinity of the blade). Thus, at least at an intuitive level, a connection is expectable between K_D and the state parameter.

- Figure 15.24(a) (Monaco et al. 2005) summarizes the various correlations developed for estimating CRR from K_D, to be used according to the "simplified procedure". Previous CRR-KD correlations were formulated by Marchetti (1982), Robertson and Campanella (1986) and Reyna and Chameau (1991) – the last one, including Imperial Valley (California) liquefaction field performance datapoints, was slightly corrected by Coutinho and Mitchell (1992) based on Loma Prieta 1989 earthquake datapoints.

- The latest CRR-K_D correlation (bold curve in Figure 15.24(a)), approximated by the equation:

$$CRR = 0.0107 K_D^3 - 0.0741 K_D^2 + 0.2169 K_D - 0.1306 \qquad (15.17)$$

It was formulated by Monaco et al. (2005) by combining previous CRR-K_D curves with the vast experience incorporated in current methods based on CPT

and SPT (supported by extensive field performance databases), translated using the relative density as intermediate parameter. This CRR-K_D curve applies to magnitude M = 7.5 earthquakes (magnitude scaling factors should be applied for other magnitudes) and "clean sand" (no further investigation into the effects of higher fines content is currently available).

- The CRR-K_D correlation by Monaco et al. (2005) was preliminarily validated by comparison with field performance datapoints from various liquefaction sites investigated after the Loma Prieta 1989 earthquake (Mw = 7), in the San Francisco Bay area, one of the few documented liquefaction cases including DMT data (reports by Coutinho and Mitchell 1992, Mitchell et al. 1994).

- Figure 15.24b shows that datapoints obtained at sites where liquefaction had occurred (mostly in hydraulic sandfills) are correctly located in the "liquefaction" side. One datapoint relevant to a non classified site, with uncertain liquefaction evidence, plots very close to the CRR-K_D boundary curve (scaled for Mw = 7).

- The convergence in a narrow band of the more recent CRR-K_D curves, compared to earlier curves, in Figure 15.24a encourages the use of K_D to estimate CRR. However, since the CRR-K_D correlation is based on a limited real liquefaction case history database, considerable additional verification is needed.

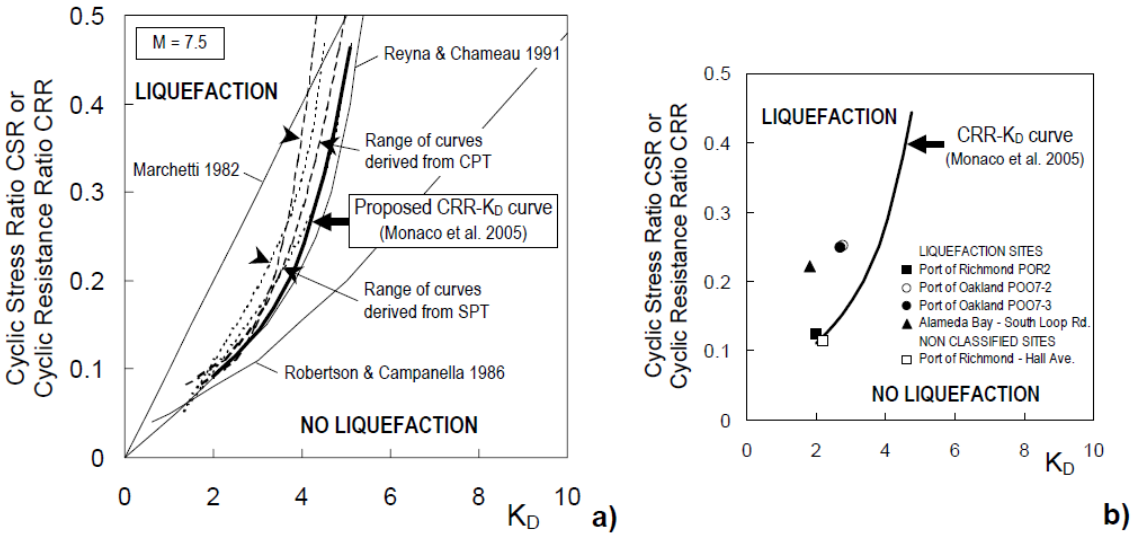

Fig 15.24: (a) CRR-K_D curves for evaluating liquefaction resistance from DMT (Monaco et al. 2005). (b) Comparison of CRR-K_D curve by Monaco et al. (2005) and Loma Prieta 1989 earthquake liquefaction datapoints (after Mitchell et al. 1994)

Topic 23

Factor of safety against liquefaction

- The final step in the liquefaction analysis is to calculate the factor of safety against liquefaction. If the cyclic stress ratio caused by the anticipated earthquake is greater than the cyclic resistance ratio of the in situ soil, then liquefaction could occur during the earthquake, and vice versa. The factor of safety against liquefaction (FS) is defined as follows:

$$FS = \frac{CRR}{CSR} \tag{15.18}$$

- The higher the factor of safety, the more resistant the soil is to liquefaction. However, soil that has a factor of safety slightly greater than 1.0 may still liquefy during an earthquake.

- For example, if a lower layer liquefies, then the upward flow of water could induce liquefaction of the layer that has a factor of safety slightly greater than 1.0. In the above liquefaction analysis, there are many different equations and corrections that are applied to both the cyclic stress ratio induced by the anticipated earthquake and the cyclic resistance ratio of the in situ soil.

- For example, there are four different corrections (that is, N_{Em}, N_b, C_v , and σ'_{v0}) that are applied to the standard penetration test N value in order to calculate the $(N_1)_{60}$ value.

- All these different equations and various corrections may provide the engineer with a sense of high accuracy, when in fact the entire analysis is only a gross approximation. The analysis should be treated as such, and engineering experience and judgment are essential in the final determination of whether a site has liquefaction potential.

Topic 24

Magnitude Scaling Factor (MSF)

- The magnitude scaling factor, MSF , has been used to adjust the induced CSR during earthquake magnitude M to an equivalent CSR for an earthquake magnitude, M = 7½. The MSF is thus defined as:

$$MSF = CSR_M / CSR_{M\,-\,7.5} \tag{15.19}$$

- Thus, MSF provides an approximate representation of the effects of shaking duration or equivalent number of stress cycles. Values of magnitude scaling factors were derived by combining:

1. Correlations of the number of equivalent uniform cycles versus earthquake magnitude,
2. Laboratory-based relations between the cyclic stress ratio required to cause liquefaction and the number of uniform stress cycles.

Anticipated Earthquake Magnitude	Magnitude Scaling Factor (MSF)
8½	0.89
7½	1.00
6¾	1.13
6	1.32
5¼	1.50

- The magnitude scaling factors plotted in Fig. below are based on
  1. Laboratory testing (Seed and Idriss 1982; Idriss 1999);
  2. Statistical analysis of observed liquefaction grouped according to discrete magnitude bins (Ambraseys 1988; Andrus and Stokoe 1997);
  3. Statistical analysis of case history data using a regression equation from which MSFs are inferred (Youd and Noble 1997);
  4. Analysis of case history data by Bayesian inference (Seed et al. 2001); and
  5. Evaluation of distant liquefaction sites from earthquakes of various magnitudes and estimates of peak accelerations at those sites (Arango 1996).

- There is significant variability in the proposed MSFs for a given m. In particular, the MSFs derived using case history data are larger than those derived using laboratory test data.

Table 15.5: Magnitude Scaling Factors

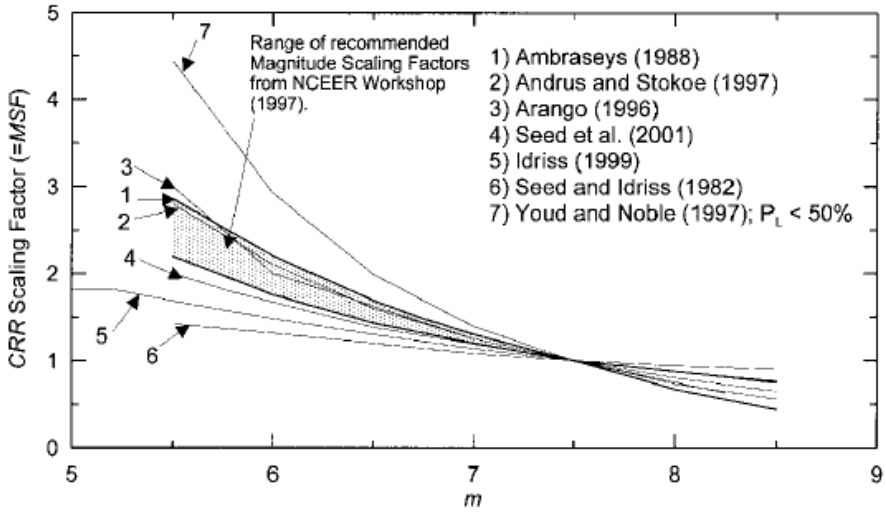

Fig 15.25: Comparison of Published CRR Weighting Factors

Topic 25

Final Choice of Factor of safety

- In evaluating the need to address the liquefaction hazards, an acceptable factor of safety needs to be chosen. Often the acceptable factor of safety is chosen arbitrarily.

- The CDMG (California Division of Mines and Geology) guidelines suggest a minimum factor of safety of 1.3 when using the CDMG ground motion maps, with a caveat that if lower values are calculated, the severity of the hazard should be evaluated.

- Clearly, no single value can be cited in a guideline, as considerable judgment is needed in weighing the many factors involved in the decision. Several of those factors are noted below:

    1. The type of structure and its vulnerability to damage.
    2. Levels of risk accepted by the owner or governmental regulations associated with questions related to design for life safety, limited structural damage, or essentially no damage.
    3. Damage potential associated with the particular liquefaction hazards. Clearly flow failures or major lateral spreads pose more damage potential than differential settlement. Hence, factors of safety could be adjusted accordingly.

4. Damage potential associated with design earthquake magnitude. Clearly a magnitude 7.5 event is potentially far more damaging than a 6.5 event.
5. Damage potential associated with SPT values, i.e., low blow counts have a greater cyclic strain potential than higher blow counts.
6. Uncertainty in SPT- or CPT- derived liquefaction strengths used for evaluations. Note that a change in silt content from 5 to 15% could change a factor of safety from say 1.0 to 1.25.
7. For high levels of design ground motion, factors of safety may be indeterminant. For example, if $(N_1)_{60}$ = 20, M = 7.5 and fines content = 35%, liquefaction strengths cannot be accurately defined due to the vertical asymptote on the empirical strength curve.

- Factors of safety in the range of about 1.1 may be acceptable for single family dwellings for example, where the potential for lateral spreading is very low and differential settlement is the hazard of concern, and where post-tensioned floor slabs are specified.

- On the other hand, factors of safety of 1.3 may be more appropriate for assessing hazards related to flow failure potential for large magnitude earthquake events.

- The final choice of an appropriate factor of safety must reflect the particular conditions associated with a specific site and the vulnerability of site related structures. Considering the high levels of seismicity in California, Table 15.6 provides a generalized guide that reflects many of the factors noted above.

Table 15.6: Factors of safety for liquefaction Hazard Assessment

Consequence of Liquefaction	$(N_1)_{60}$ (clean sand)	Factor of safety
Settlement	≤15	1.1
	≥30	1.0
Surface Manifestation	≤15	1.2
	≥30	1.0
Lateral Spread	≤15	1.3
	≥30	1.0

- These factors of safety remain open for discussion. Within the Implementation Committee, there was not a complete consensus on these factors of safety; a minority position favors setting the factors of safety in the range between 1.25 and 1.5.

Topic 26

Zone of Liquefaction

- The State Geologist is required under the Seismic Hazards Mapping Act of 1991 to delineate various "seismic hazard zones," including those for liquefaction. The criteria for delineating Liquefaction Zones were developed by the Seismic Hazards Mapping Act Advisory Committee for the California State Mining and Geology Board in 1993, and will be contained in a revised document entitled "Guidelines For Delineating Seismic Hazard Zones" (CDMG, 1999).

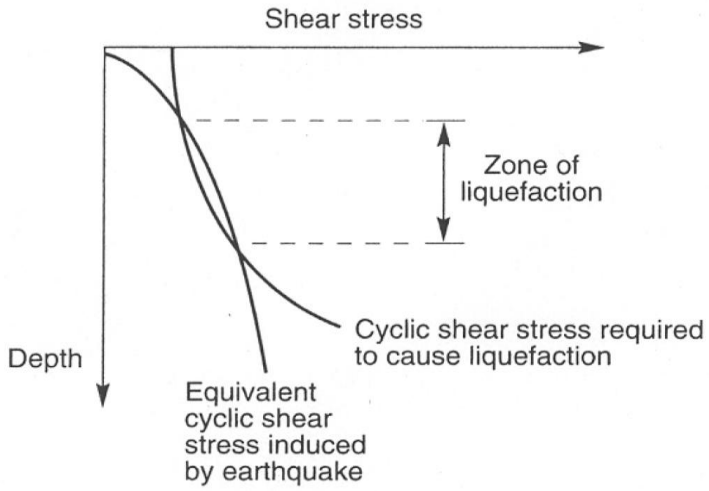

Fig 15.26: Shear Stress Vs. Depth

- Under those criteria, Liquefaction Zones are areas meeting one or more of the following:

1. Areas where liquefaction has occurred during historical earthquakes.
2. Areas of uncompacted or poorly compacted fills containing liquefaction-susceptible materials that are saturated, nearly saturated, or may be expected to become saturated.
3. Areas where sufficient existing geotechnical data and analyses indicate that the soils are potentially susceptible to liquefaction.
4. For areas where geotechnical data are lacking or insufficient, zones are delineated using one or more of the following criteria:
    a) Areas containing soil of late Holocene age (less than 1,000 years old, current river channels and their historical flood plains, marshes, and estuaries) where the groundwater is less than 40 feet deep and the anticipated earthquake peak ground acceleration (PGA) having a 10% probability of being exceeded in 50 years is greater than 0.1g.

b) Areas containing soils of Holocene age (less than 11,000 years old) where the groundwater is less than 30 feet below the surface and the PGA (10% in 50 years) is greater than 0.2g.
c) Areas containing soils of latest Pleistocene age (11,000 to 15,000 years before present) where the groundwater is less than 20 feet below the surface and the PGA (10% in 50 years) is greater than 0.3g.

- It should be noted that the groundwater levels used for the purposes of zoning are the historically shallowest (highest) groundwater levels using the results of groundwater studies.

- Sediments deposited on canyon floors are presumed to become saturated during wet seasons and shallow water conditions can occur in narrow stream valleys that can receive an abundance of water runoff from canyon drainages and tributary streams during periods of high precipitation.

Topic 27

Liquefaction Potential Index

- Iwasaki et al. (1978) developed the liquefaction potential index (LPI) to predict the potential of liquefaction to cause foundation damage at a site. They assumed that the severity of liquefaction should be proportional to the

1. Thickness of the liquefied layer;
2. Proximity of the liquefied layer to the surface; and
3. Amount by which the factor safety (FS) is less than 1.0,

- where FS is the ratio of the liquefaction resistance to the load imposed by the earthquake. Because surface effects from liquefaction at depths greater than 20 m are rarely reported, they limited the computation of LPI to depths (z) ranging from 0 to 20 m. They proposed the following definition:

$$LPI = \int_0^{20m} Fw(z)dz \qquad (15.20)$$

In which $F = 1 - FS$ *for* $FS \le 1$, and

$F = 0$ *for* $FS > 1$

Depth weighting factor, w(z)=10-0.5z

- where z=depth in meters. By this definition, values of LPI can range from 0 for a site with no liquefaction potential to a maximum of 100 for a site where the factor of safety is zero over the entire 20-m-depth range.

- Fig. 15.27 is an example calculation of LPI for a CPT sounding at a location subjected to two different earthquake loadings. In practice with CPT measurements, the integral in avove Eq. is replaced with a summation of depth increments equal to the sampling interval of the CPT.

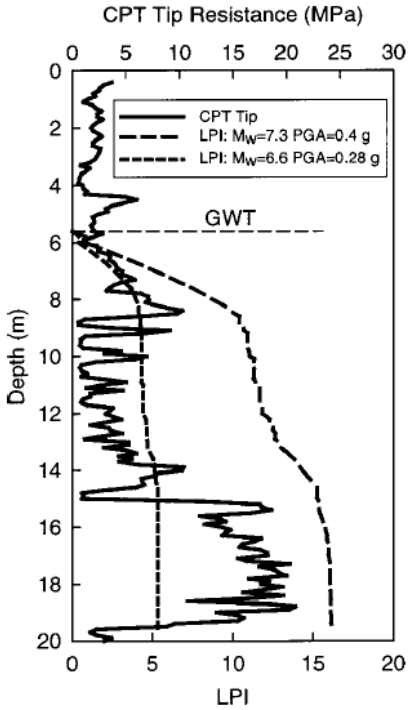

Fig 15.27: Example calculation of LPI with a CPT sounding for two earthquakes: An M_W 6.6 and 7.3, respectively, with peak ground accelerations (PGA) of 0.28 and 0.4 g

- To compute LPI, depth intervals with materials susceptible to liquefaction are first inferred from the CPT tip and sleeve friction. Then factors of safety against liquefaction are computed for susceptible material.

- Fig. 15.27 shows the accumulation of LPI with depth, i.e., the partial integral of above Eq., for two different earthquakes: an MW 6.6 and MW 7.3 with peak ground accelerations of 0.28 and 0.4 g, respectively.

- Note that the MW 7.3 earthquake produces an LPI of 16, the value at 20 m, which is substantially larger than the LPI of about 5 produced by the MW 6.6 earthquake. The example also illustrates how the contribution to LPI may vary significantly with depth. In the example, most of the LPI contribution is from the sandy interval between 6 and 9 m.

- LPI has not been widely applied in field investigations primarily because of both the limited evaluations and calibrations of the LPI scale and the need for detailed information on the thickness of susceptible layers and their liquefaction

resistance. Iwasaki et al. (1982) conducted the most thorough effort to calibrate the significance of numerical values of LPI.

- They evaluated LPI at 85 sites in Japan for six earthquakes. Of the 85 sites, 63 showed evidence of liquefaction and 22 did not. It is unclear from their publication whether ‘‘site’’ refers to a single standard penetration test boring or is an average of multiple borings within an area, but it appears they were using individual borings.

- Their calculated LPI values were based on SPT blow counts, which typically are measured at a 1-m spacing in Japan. They concluded that severe liquefaction is likely at sites with LPI.15 and is not likely at sites with LPI,5. Other attempts to relate LPI values to liquefaction severity are more modest.

- Chameau et al. (1991) conducted cone penetration testing at six sites underlain by artificial fill that liquefied during the 1989 Loma Prieta, Calif., earthquake. They concluded that LPI captured the relative risk of the six sites. Luna and Frost (1998) used LPI to map variations of liquefaction potential on Treasure Island, a hydraulic fill in San Francisco Bay, Calif., and compared the values to damage. Table 15.8 shows the Liquefaction potential classification proposed by Sonmez (2003)

Table 15.7: Liquefaction potential classification proposed by Sonmez (2003)

Liquefaction Potential Index (L_I)	Liquefaction potential category
0	Non- liquefiable (based on FS ≥1.2)
$0< L_I \leq 2$	Low
$2< L_I \leq 5$	Moderate
$5< L_I \leq 15$	High
$15 > L_I$	Very high

Topic 28

Liquefaction Severity Index

- Determination of factor of safety against liquefaction using deterministic method is not the best judgment of whether liquefaction occurred in a post-earthquake investigation due to an unknown degree of conservatism (Yuan et al. 2003).

- The probabilities of soil liquefaction depending on factor of safety values are preformed by Chen and Juang (2000) and Juang et al. (2003). Equation for the probability of liquefaction is proposed by Juang et al. (2003) and probability of liquefaction (PL) ranges from zero to one as a function of factor of safety.

- Original equations and the likelihood of liquefaction of a soil layer classification are discussed in Sonmez and Gokceoglu, (2005). Lee et al. (2003) proposed liquefaction risk index (IR) by combining Juang et al. (2003) and Iwasaki et al (1982). Sonmez and Gokceoglu, (2005) presented the limitations and alternate name for liquefaction risk index. Sonmez and Gokceoglu, (2005) proposed the revised probabilities of soil liquefaction depending on factor of safety values called liquefaction severity index (L_S) and its classification.

- In this study liquefaction severity index (L_S) has been calculated to identify the probability of liquefaction potential using the method proposed by Sonmez and Gokceoglu, (2005). The proposed equations by Sonmez and Gokceoglu, (2005) for the determination of L_S are given below:

$$L_S = \int_0^{20} P_L(z) W(z) dz \tag{15.21}$$

$$P_L(z) = \frac{1}{1 + \left(FS / 0.96\right)^{4.5}} \quad for\ FS \le 1.411 \tag{15.22}$$

$$P_L(z) = 0 \quad for\ FS \succ 1.411 \tag{15.23}$$

- The soil layer with FL 1:411 can be considered as non-liquefiable layer considering clay content and liquid limit. The liquefaction severity index (LS) is calculated and classified according to new liquefaction severity classification suggested by Sonmez and Gokceoglu, (2005).

- Table 15.8 shows the Liquefaction severity classification suggested by Sonmez and Gokceoglu, (2005). Figure 15.28 shows liquefaction severity map of Bangalore. This study shows that major part of Bangalore under non liquefiable category having LS as 0. Few locations in the northern part of study area have very low liquefaction probability and portion of study area in western part has low to moderate liquefaction probability for post earthquakes.

Table 15.8: Liquefaction severity classification proposed by Sonmez and Gokceoglu, (2005)

Liquefaction severity Index (Ls)	Description
$85 \leq L_S < 100$	Very High
$65 \leq L_S < 85$	High
$35 \leq L_S < 65$	Moderate
$15 \leq L_S < 35$	Low
$0 < L_S < 35$	Very Low
$L_S = 0$	Non liquefied

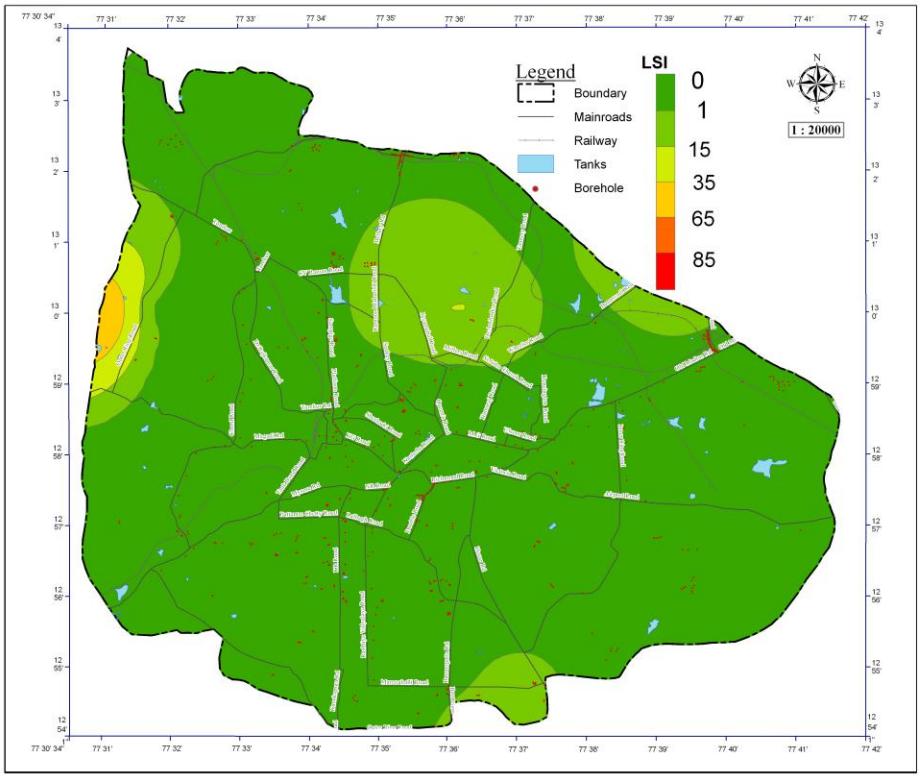

Figure 15.28: Liquefaction severity map of Bangalore

Topic 29

Probabilistic evaluation of seismic liquefaction potential

- The methods suggested by Seed and Idriss (1971) and Cetin et al. (2002) for evaluating liquefaction potential do not consider the uncertainty in the earthquake loadings.
- Kramer and Mayfield (2007) incorporated the probabilistic method suggested by Cetin et al. (2002) into a performance-based analysis to evaluate the return period of seismic soil liquefaction.

- In this approach, the contributions from all magnitudes and all acceleration levels are considered. Thus, the uncertainty in the earthquake loading for the initiation of liquefaction is explicitly included in the analysis. This is achieved by discretizing the seismic hazard ''space'' into a large number of acceleration and magnitude bins.

- Thus instead of taking a single acceleration and earthquake magnitude, as in the conventional approach, it covers the entire acceleration and earthquake magnitude ranges. This method is formulated based on the probabilistic framework by Kramer and Mayfield (2007).

$$\lambda_{EDP^*} = \sum_{i=1}^{N_{IM}} P\left[EDP > EDP^* \middle| \mathrm{IM} = \mathrm{im_i} \right] \Delta\lambda_{im_i} \tag{15.24}$$

- Where *EDP* – Engineering damage parameter like factor of safety etc.; EDP^* - a selected value of *EDP*; *IM* – intensity measure which is used to characterize the earthquake loading like peak ground acceleration, etc; $\mathrm{im_i}$ – the discretized value of *IM*; λ_{EDP^*} - mean annual rate of exceedance of EDP^*; $\Delta\lambda_{im_i}$ - incremental mean annual rate of exceedance of intensity measure *im*. The following equation can be derived by considering the *EDP* as factor of safety and the intensity measure of ground motion as a combination of PGA and magnitude.

$$\Lambda_{FS_L^*} = \sum_{j=1}^{N_M} \sum_{i=1}^{N_a} P[\mathrm{FS_L} < \mathrm{FS_L^*} \mid \mathrm{a_i}, m_j] \Delta\lambda_{a_i, m_j} \tag{15.25}$$

- Where $\Lambda_{FS_L^*}$ - annual rate at which factor of safety will be less than $\mathrm{FS_L^*}$; FS_L – factor of safety against liquefaction; $\mathrm{FS_L^*}$ - targeted value of factor of safety against liquefaction; N_M - Number of magnitude increments; N_a - number of peak acceleration increments; $\Delta\lambda_{a_i, m_j}$ - incremental annual frequency of exceedance for acceleration a_i and magnitude m_j (this value is obtained from the deaggregated seismic hazard curve with respect to magnitude). The conditional probability in Eq. (15.25) is (Kramer and Mayfield, 2007).

$$\mathrm{P[FS_L < FS_L^* \mid a_i, m_j]} = \Phi\left[-\frac{(N_1)_{60}(1+\theta_1 FC) - \theta_2 \ln(CSR_{eq,i} FS_L^*) - \theta_3 \ln(m_j) - \theta_4 (\ln(\sigma'_{v0} / P_a) + \theta_5 FC + \theta_6}{\sigma_\varepsilon} \right] \tag{15.26}$$

Where Φ – standard normal cumulative distribution; $(N_1)_{60}$ – resistance of the soil from the Standard Penetration Test corrected for energy and overburden pressure; *FC* – fines content of the soil in percent; σ'_{v0} - effective over burden pressure; P_a – atmospheric pressure in the same unit as σ'_{v0}; θ_i and σ_ε – model coefficients developed by regression.

$$CSR_{eq,i} = 0.65 \frac{a_i}{g} \frac{\sigma_{vo}}{\sigma'_{vo}} r_d \qquad (15.27)$$

$CSR_{eq,i}$, the *CSR* value calculated without using the MSF for an acceleration a_i, will be calculated for all the acceleration levels. The most widely used technique to calculate the stress reduction factor (r_d) is suggested by Seed and Idriss (1971). Further, Cetin and Seed (2004) evolved a method to evaluate the stress reduction factor as a function of depth, earthquake magnitude, ground acceleration and the average shear wave velocity of the top 12 m soil column. For a depth < 20 m:

$$r_d(d, Mw, a_{\max}, V^*_{s,12}) = \frac{\left[1 + \frac{-23.013 - 2.949a_{\max} + 0.999M_w + 0.0525V^*_{s,12}}{16.258 + 0.201e^{0.341(-d + 0.0785V^*_{s,12} + 7.586)}}\right]}{\left[1 + \frac{-23.013 - 2.949a_{\max} + 0.999M_w + 0.0525V^*_{s,12}}{16.258 + 0.201e^{0.341(0.0785V^*_{s,12} + 7.586)}}\right]} \pm \sigma_{\varepsilon_{r_d}}$$

(15.28)

Where a_{max} and M_w are the maximum acceleration (in g) and corresponding earthquake moment magnitude value; $V^*_{s,12}$ - average shear wave velocity in m/s for the top 12 m soil layer and the values for $\sigma_{\varepsilon_{r_d}}$ is the standard deviation of model error.

- The Eq. 5 is developed for a single earthquake magnitude and acceleration. Since the discretized magnitude (m_j) and acceleration (a_i) ranges are considered for calculation in Eq. 3 and 4, the above equation for calculating r_d has been modified in this study to account for all the acceleration and magnitude values:

- $$r_d(d, m_j, a_i, V^*_{s,12}) = \frac{\left[1 + \frac{-23.013 - 2.949a_i + 0.999m_j + 0.0525V^*_{s,12}}{16.258 + 0.201e^{0.341(-d + 0.0785V^*_{s,12} + 7.586)}}\right]}{\left[1 + \frac{-23.013 - 2.949a_i + 0.999m_j + 0.0525V^*_{s,12}}{16.258 + 0.201e^{0.341(0.0785V^*_{s,12} + 7.586)}}\right]} \qquad (15.29)$$

- Where a_i and m_j correspond to the discretized acceleration and magnitude values. Based on the shear wave velocity value available for the study area, the value of $V^*_{s,12}$ was calculated as 220 m/s using the following equation.

$$V^*_{s,12} = \frac{12}{\sum \frac{d_i}{V_{s_i}}} \qquad (15.30)$$

Where V_{s_i} - Shear wave velocity at a depth d_i and d_i <= 12 m

- As an alternative to FS_L, liquefaction potential can be characterized by the SPT resistance required to prevent liquefaction, N_{req}, at a given location in the site and at a required depth. The probabilistic method can be applied to get the annual frequency of exceedance for N^*_{req} :

$$\lambda_{N^*_{req}} = \sum_{j=1}^{N_M} \sum_{i=1}^{N_a} P[N_{req} > N^*_{req} \mid a_i, m_j] \Delta\lambda_{a_i, m_j} \quad (15.31)$$

Where

$$P[N_{req} > N^*_{req} \mid a_i, m_j] = \Phi\left[-\frac{N^*_{req} - \theta_2 \ln(CSR_{eq,i}) - \theta_3 \ln(m_j) - \theta_4 (\ln(\sigma'_{v0} / P_a) + \theta_6}{\sigma_\varepsilon} \right] \quad (15.32)$$

The value of N^*_{req} is the corrected N value (for both over burden pressure and percentage of fines) required to prevent the liquefaction with an annual frequency of exceedance of $\lambda_{N^*_{req}}$. More details about probabilistic approach liquefaction can be found Vipin et al (2010).

Lecture 15 Introduction to Liquefaction; Mechanism and factors causing liquefaction; estimation methods and procedures; Mapping